

Highlights

Payoff scaling shapes cooperation in LLM agents across languages

Trung-Kiet Huynh, Dao-Sy Duy-Minh, Thanh-Bang Cao, Phong-Hao Le, Hong-Dan Nguyen, Phu-Quy Nguyen-Lam, Minh-Luan Nguyen-Vo, Hong-Phat Pham, Phu-Hoa Pham, Thien-Kim Than, Chi-Nguyen Tran, Huy Tran, Gia-Thoai Tran-Le, Alessio Buscemi, Le Hong Trang, The Anh Han

- Payoff-scaled iterated prisoner's dilemma framework isolates LLM sensitivity to incentive stakes.
- Higher payoff stakes shift LLMs from defection toward cooperative strategies.
- Evolutionary game theory baseline contrasts predicted vs. observed LLM strategy mixes.
- Linguistic framing rivals model architecture in shaping LLM strategic behaviour.
- Open-weight small LLM replication confirms the generality of incentive and language effects.
- Diagnostic toolkit for AI governance of multi-agent language-model systems.

Payoff scaling shapes cooperation in LLM agents across languages

Trung-Kiet Huynh^{a,c,1}, Dao-Sy Duy-Minh^{a,c,1}, Thanh-Bang Cao^{b,c}, Phong-Hao Le^{b,c},
Hong-Dan Nguyen^{b,c}, Phu-Quy Nguyen-Lam^{a,c}, Minh-Luan Nguyen-Vo^{b,c}, Hong-Phat Pham^{b,c},
Phu-Hoa Pham^{a,c}, Thien-Kim Than^{b,c}, Chi-Nguyen Tran^{b,c}, Huy Tran^{b,c}, Gia-Thoai Tran-Le^{b,c},
Alessio Buscemi^d, Le Hong Trang^{b,c,*} and The Anh Han^{e,*}

^aFaculty of Information Technology, University of Science (HCMUS), Ho Chi Minh City, Vietnam

^bFaculty of Computer Science and Engineering, Ho Chi Minh City University of Technology (HCMUT), Ho Chi Minh City, Vietnam

^cVietnam National University – Ho Chi Minh City (VNU-HCM), Ho Chi Minh City, Vietnam

^dLuxembourg Institute of Science and Technology (LIST), Luxembourg

^eSchool of Computing, Engineering and Digital Technologies, Teesside University, Middlesbrough, United Kingdom

ARTICLE INFO

Keywords:

Large Language Models
Multi-agent systems
Cooperation
Evolutionary Game Theory
Iterated Prisoner's Dilemma
Cross-lingual behaviour
Supervised intention recognition

ABSTRACT

Large language models (LLMs) are increasingly deployed as autonomous agents that negotiate, coordinate, and act on behalf of users. Whether they cooperate in such settings is no longer just an academic question, but a central issue for AI governance. We approach it from a strategic-behaviour angle, asking how two everyday levers – the size of what is at stake, and the language in which the interaction is described – shape the strategies LLMs adopt in a repeated Prisoner's Dilemma. Rather than reading cooperation off raw action counts, we train supervised classifiers to recognise the canonical strategies of repeated games (always cooperate, always defect, Tit-for-Tat, Win-Stay-Lose-Shift) and use them as a lens onto LLM behaviour. To know what the strategy distribution *should* look like under the same payoffs, we derive an evolutionary game theory (EGT) baseline and compare it with the LLM data. The two outcomes disagree in a revealing way: as stakes grow, evolutionary theory predicts that defection should take over the population, yet LLMs move in the opposite direction, becoming more cooperative – a signature, we argue, of alignment training and the human-like reasoning patterns LLMs inherit from their training data. We further show that this picture is not particular to frontier-scale, proprietary models: it also occurs with three open-weight smaller LLMs. Overall, our analysis highlights that payoff design and linguistic framing are powerful but under-explored levers for steering LLM behaviour, with direct implications for evaluating, aligning, and governing multi-agent AI systems deployed in high-stakes, multilingual environments.

1. Introduction

Large language models (LLMs) are increasingly deployed as *agents* in recommendation systems, negotiation tools, and multi-agent assistants [12, 21, 53]. In these settings, LLMs face *cooperation dilemmas* in which behaviour emerges from strategic interactions rather than isolated model outputs. Empirical studies show that such behaviour is shaped by training, prompting, role assignment, and linguistic framing, with direct implications for safety, coordination, and AI governance [1, 17, 22, 30, 39]. Equally critical is the adaptability of their cooperative strategies to varying costs and benefits (payoff stakes), as this directly influences AI system outcomes across a spectrum of real-world scenarios [21].

A growing body of work evaluates LLMs through game-theoretic lenses, particularly via matrix and repeated games, revealing systematic departures from Nash equilibria, persistent cooperative biases, and sensitivity to contextual factors such as language and incentives [1, 10, 16, 18, 40, 45, 46, 51, 55]. These studies increasingly rely on controlled experimental testbeds that vary models, languages, payoff structures, and agent roles. Yet most existing evaluations

*Corresponding author.

Email addresses: 23122039@student.hcmus.edu.vn (T.K. Huynh); 23122041@student.hcmus.edu.vn (D.S. Duy-Minh); bang.caothanh455@hcmut.edu.vn (T.B. Cao); hao.lephong@hcmut.edu.vn (P.H. Le); nhdan.sdh232@hcmut.edu.vn (H.D. Nguyen); 23122048@student.hcmus.edu.vn (P.Q. Nguyen-Lam); luan.nguyenvm@hcmut.edu.vn (M.L. Nguyen-Vo); phat.phamhong@hcmut.edu.vn (H.P. Pham); 23122030@student.hcmus.edu.vn (P.H. Pham); kim.thanthien04@hcmut.edu.vn (T.K. Than); 23122044@student.hcmus.edu.vn (C.N. Tran); tranhuy@hcmut.edu.vn (H. Tran); thoai.trantlgt2610@hcmut.edu.vn (G.T. Tran-Le); alessio.buscemi@list.lu (A. Buscemi); lhtrang@hcmut.edu.vn (L.H. Trang); t.han@tees.ac.uk (T.A. Han)

ORCID(s):

¹These authors contributed equally to this work.

still focus on aggregate outcomes—such as cooperation rates or payoff distributions—and do not directly model the *behavioural intentions* underlying observed actions.

Evaluating strategic behaviour at the level required for governance and alignment therefore demands methods that go beyond surface-level outputs. Drawing on behavioural and evolutionary game theory [50], we conceptualise behavioural intention as an agent’s *strategy*: a decision rule mapping interaction histories to subsequent actions [14, 19, 23, 24]. Classical canonical strategies in repeated games, such as Always Cooperate (ALLC), Always Defect (ALLD), Tit-for-Tat (TFT), and Win-Stay–Lose-Shift (WSLS) [4, 50], provide an interpretable vocabulary for such intentions. Prior work has shown that these strategies can be inferred from noisy behavioural trajectories using supervised learning [14, 23], and extended using probabilistic models to capture mixed or stochastic behaviour [42].

In parallel, recent studies highlight that LLM behaviour is not invariant across languages [10]. Strategic reasoning, risk sensitivity, and cooperation patterns have been shown to depend on linguistic framing, sometimes with effects comparable in magnitude to architectural differences [9, 37]. This raises the question of whether behavioural intentions (or strategies used by LLM agents) inferred from gameplay are themselves language-dependent, and whether such dependencies introduce systematic biases in multi-agent settings.

This work builds on and extends these strands of research. Our experimental design incorporates a payoff-scaled Prisoner’s Dilemma that systematically varies the *stakes* (i.e. magnitude) of cooperation while preserving the underlying strategic structure. Moreover, using synthetic repeated-game trajectories [23], we train supervised intention classifiers and apply them to LLM-generated gameplay logs to infer canonical strategies. To anchor the empirical findings to a theoretical benchmark, we additionally compute the stationary distribution of canonical strategies under the same payoff structure using a finite-population evolutionary game theory (EGT) model, and contrast the EGT predictions with the LLM-derived frequencies. This setup is in the spirit of recent work that combines EGT modelling with LLM-based simulations to study strategic behaviour in social and governance dilemmas [7, 9]. To further test the generality of the framework, we replicate the payoff-scaled protocol on three open-weight small LLMs. Together, these elements allow us to address three important questions:

- (1) Do LLM agents systematically change cooperative behaviour as payoff stakes vary, and how does this differ across models and languages?
- (2) Can LLM behavioural intentions be reliably classified using supervised learning, and what systematic biases emerge across models and languages?
- (3) How do the LLM-derived strategy distributions compare with the EGT baseline under matched payoff and noise conditions, and to what extent do these patterns generalise to smaller, open-weight LLMs?

Our approach complements and extends recent long-horizon studies of repeated games with LLMs. In particular, Fontana et al. [17] analyse 100-round interactions and introduce the Strategy Frequency Estimation Method (SFEM) to recover rich strategic archetypes, including Grim Trigger, Generous Tit-for-Tat, and extortionate strategies, achieving high population-level accuracy. Our approach employs a 10-round horizon, which is designed to enable direct exploration of payoff-scaling and multilingual effects – the core contextual factors of our study. This design, while trading off the capacity to discern complex, multi-stage conditional strategies, allows us to obtain highly interpretable, pointwise estimates of canonical intentions. The EGT baseline plays a complementary role: by deriving the long-run frequency of each canonical strategy under the same payoff matrix as a function of stake magnitude and execution noise, it characterises which strategy mixtures are evolutionarily stable in the underlying game, and thus identifies the directions in which the LLM-derived distributions agree with or depart from the game-theoretic prediction [7, 25, 50].

Finally, while human behavioural baselines in repeated Prisoner’s Dilemma are well studied [1, 4, 33, 42, 50], systematic comparisons under matched experimental conditions remain largely absent from LLM evaluations. Human cooperation rates and strategy distributions vary with incentives, culture, and framing. Our findings of incentive- and payoff-stakes-sensitive cooperation and cross-linguistic divergence echo these patterns, but without direct human baselines we do not claim behavioural equivalence. Instead, we position intention classification as a diagnostic tool for identifying systematic structure and bias in LLM strategic behaviour, providing a foundation for future comparative and governance-oriented analyses.

Our experiments build on FAIRGAME – the Framework for AI Agents Bias Recognition using Game Theory [10] – providing a controlled experimental testbed for probing these effects across models, languages and personalities. The FAIRGAME-based studies [7, 10, 11] does not include a payoff-scaling protocol, an EGT comparator, or a supervised intention-recognition layer. The contributions of the present paper are: **(i)** the payoff-scaled, finite-horizon protocol

introduced in Section 2.2; **(ii)** the supervised, hybrid (LSTM + rule) intention-recognition pipeline applied to LLM-generated trajectories (Section 2.3); **(iii)** the analytical evolutionary game baseline placed alongside the empirical LLM distributions under matched payoff and noise conditions (Sections 3.4 and 3.5); and **(iv)** an open-weight replication that confirms the qualitative findings on three smaller models (Section 3.6).

2. Methodology

2.1. Framework

FAIRGAME (Framework for AI Agents Bias Recognition using Game Theory) [10] provides our computational infrastructure. The framework supports systematic, reproducible LLM evaluations through controlled game-theoretic experiments. Experimental conditions are defined via JSON configuration files specifying payoff structures, game horizon, LLM backends, and languages. At runtime, FAIRGAME combines configurations with language-specific prompt templates, simulates repeated normal-form games, and logs round-by-round trajectories. We extend FAIRGAME with payoff-scaling for the Prisoner’s Dilemma to investigate LLM sensitivity to incentive magnitude.

2.2. Payoff stakes: scaled payoff matrix

We first examine the sensitivity of LLM agents to the absolute magnitude of incentives in a dyadic setting. To this end, we use a repeated Prisoner’s Dilemma in which only the numerical values of the payoffs are scaled, while the underlying strategic structure of the game is kept fixed. In this way, the “stakes” of the interaction are varied without changing best responses or the ranking of outcomes. It has been shown, theoretically [25] and empirically in human experiments [33, 34], that cooperative behaviours are strongly influenced by this factor. This design connects to recent work on workflow-guided rationality and opponent shaping in LLM agents [28], where stake magnitude may interact with learned policies to produce non-trivial behavioural shifts.

The row player’s baseline payoff matrix is given by $((A, A) \mapsto (6, 6), (A, B) \mapsto (0, 10), (B, A) \mapsto (10, 0), (B, B) \mapsto (2, 2))$, where Option A denotes defection and Option B cooperation. The agents’ objective is to *minimise* their cumulative penalties. Thus, mutual cooperation (B, B) yields the lowest combined penalty $(2, 2)$, while mutual defection (A, A) yields higher penalties $(6, 6)$. Under the penalty framing, the matrix satisfies the ordering $T(0) < R(2) < P(6) < S(10)$, where T (Temptation: defecting while opponent cooperates) yields the lowest penalty, followed by R (Reward: mutual cooperation), P (Punishment: mutual defection), and S (Sucker: cooperating while opponent defects). Note that in standard reward framing, the ordering is inverted ($T > R > P > S$); our penalty framing preserves the PD incentive structure where defection is individually dominant. To manipulate the stakes of the game without altering its strategic structure, we introduce a scalar parameter $\lambda > 0$ and multiply all penalties by λ [25]. In our experiments we consider three values - $\lambda \in \{0.1, 1.0, 10.0\}$ - corresponding to attenuated, baseline, and amplified payoff magnitudes (e.g., mutual cooperation yields penalties of 0.2, 2, and 20 respectively). The payoff ordering is preserved in all cases, isolating the effect of payoff magnitude while keeping the underlying game-theoretic incentives unchanged. Scaled payoff matrix examples for each λ value are provided in Appendix A.2.

Two-player games between LLM agents are run using FAIRGAME as the simulation engine [10]. Each game is played for a fixed, finite horizon of $N = 10$ rounds; following the known-horizon condition from the FAIRGAME protocol, agents are explicitly informed of the total number of rounds in the prompt, which may drive end-game defection patterns consistent with backward induction in finite repeated games [50]. End-game effects are evident: defection rates in rounds 9–10 exceed those in rounds 1–8 across most conditions, consistent with backward-induction reasoning (Claude 3.5 Haiku at high stakes is a notable exception, where cooperative learning persists into the final rounds). The unknown-horizon condition, where agents are not informed of the game length, remains an avenue for future investigation. In every round both agents observe the full public history of past actions and payoffs before choosing their next move. Agents do not communicate outside of their action choices. For each parameter configuration, we simulate multiple independent runs (10 repetitions per condition) to account for the stochasticity of LLM outputs. We evaluate three LLM backends: GPT-4o [29] (temperature: 1.0, top_p: 1.0), Claude 3.5 Haiku [3] (temperature: 1.0, top_p: 1.0), and Mistral Large [41] (temperature: 0.3, top_p: 1.0). Following the FAIRGAME protocol [10], we adopt each provider’s recommended default settings rather than standardising across models. This design choice reflects realistic deployment conditions: practitioners typically use models “out of the box” with vendor-recommended configurations, and our behavioural findings thus generalise to practical multi-agent applications. While temperature differences (GPT-4o/Claude: 1.0; Mistral: 0.3) may introduce variability confounds, prior FAIRGAME analyses demonstrate that key behavioural patterns (cross-linguistic divergence, personality effects) persist across models

despite differing temperature settings; controlled temperature ablations remain an avenue for future work. Complete LLM configuration details (model versions, API parameters, and system prompts) are documented in Appendix A.1.

To examine potential cross-lingual effects, the same game is instantiated in five languages: English, French, Arabic, Mandarin Chinese, and Vietnamese. Prompt templates were translated by native speakers with back-translation verification to ensure semantic and numeric equivalence across languages; all templates explicitly instruct agents that lower penalties are better outcomes, verified through independent review by native speakers to avoid misinterpretation; templates will be released with the code. Agent roles (first/second mover) were randomised across runs to control for positional bias. In all conditions, neutral framing is employed: “Option A” corresponds to defection and “Option B” to cooperation, and the prompt does not contain any explicit moral or normative language. Personality traits, cooperative (C) or selfish (S), are systematically varied across agent pairings (CC, CS, SC, SS). In total, we run 3 models \times 5 languages \times 3 λ values \times 4 personality pairings \times 10 repetitions = 1,800 games, yielding 36,000 agent decisions (each game produces 20 decisions across $N=10$ rounds for 2 agents). A complementary replication with three open-weight small models extends this to $N=30$ rounds and six multipliers ($\lambda \in \{0.01, 0.1, 1, 10, 100, 1000\}$); its full protocol and results are reported in Section 3.6.

2.3. LLM behavioural intention recognition

While the FAIRGAME framework provides complete gameplay trajectories and descriptive metrics such as cooperation rates and payoff sensitivities, these primarily capture what agents do rather than why they behave that way. Our goal is to uncover the latent behavioural intentions embedded within these decision sequences to better interpret the motivations behind agents’ actions and understand how LLM strategies differ from human strategies.

Building on prior work by Han et al. [23, 24] and Di Stefano et al. [14], which demonstrated how to infer canonical strategies from large-scale repeated gameplay data by incorporating execution noise (ϵ) to replicate stochasticity, we adopted and adapted this methodology. Our objective is to apply this approach to classify the underlying behavioural intentions exhibited by LLMs during their gameplay turns. Figure 1 illustrates the pipeline we employed, detailing how this intention prediction model was adapted to analyse the outputs of the FAIRGAME framework.

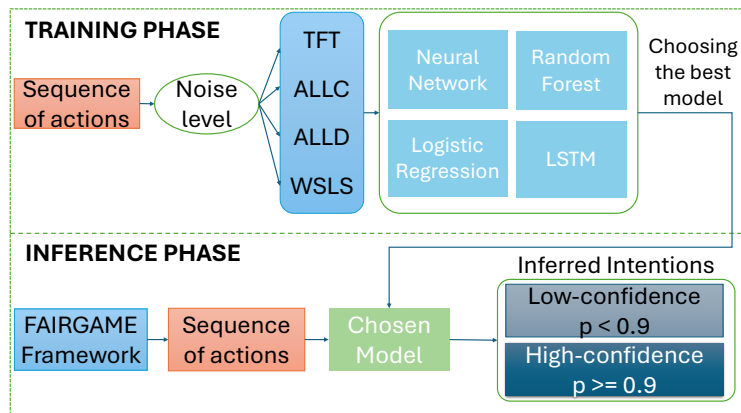


Figure 1: Supervised learning pipeline for understanding LLM behaviour. Starting from action sequences associated with canonical strategies (ALLC, ALLD, TFT, WSLS) under varying noise conditions, we train supervised learning models to infer and classify underlying behavioural intentions. We then apply the best-performing model to the LLM repeated-gameplay data generated by FAIRGAME. High-confidence predictions (> 0.9) are used to identify which strategies the LLM adopts, whereas low-confidence cases are reserved for subsequent analysis to investigate the possibility of emerging behaviours by the LLM.

Following [14], we generate 10,000 synthetic trajectories (2,500 per strategy, balanced) for four canonical strategies: TFT, ALLC, ALLD, and WSLS [50] (see Appendix A.3 for formal definitions). Each trajectory spans 10 rounds against a random opponent, with execution noise ($\epsilon \in \{0, 0.05\}$) injected to simulate LLM stochasticity. We train Logistic Regression [13], Random Forests [8], feed-forward Neural Networks [32], and Long Short-Term Memory (LSTM) recurrent networks [27] as candidate classifiers, selecting the best-performing model – the LSTM – for downstream inference because it can exploit the sequential structure of the action history. The choice matters: a static classifier treats each round in isolation, whereas a recurrent network can “remember” that the agent has, say,

just been double-crossed three times in a row, which is exactly the kind of information a canonical conditional strategy uses.

FAIRGAME logs are preprocessed into state-action sequences encoding interaction outcomes: Reward (R), Punishment (P), Temptation (T), and Sucker (S). The trained model outputs probability distributions over strategy classes; we focus on high-confidence predictions (> 0.9) to ensure reliability.

3. Results

3.1. Payoff magnitude sensitivity

The results in this subsection are based on the payoff-scaled Prisoner’s Dilemma experiments described in Section 2.2. These experiments evaluate three LLM models (GPT-4o, Claude 3.5 Haiku, and Mistral Large) across five languages (Arabic, Chinese, English, French, and Vietnamese) under three payoff scaling conditions ($\lambda \in \{0.1, 1.0, 10.0\}$). Following the FAIRGAME framework [10], the payoff matrix represents *penalties* (years of imprisonment in the Prisoner’s Dilemma narrative), where lower values indicate better outcomes for agents. The agents’ objective is to *minimise* their cumulative penalties over the course of the repeated game.

Figure 2 summarises the cooperative behaviour of the three proprietary LLMs across the payoff sweep. The two panels report the *cooperation rate* – the percentage of rounds in which an agent picked Option B (cooperate) – as a function of the stake multiplier λ , broken down (a) by model and (b) by prompt language. Lines are means across all games for a given cell; error bars are standard errors over games. The detailed per-(language, pairing, model) penalty grid that this figure summarises is reported in Appendix B.1.4 for completeness.

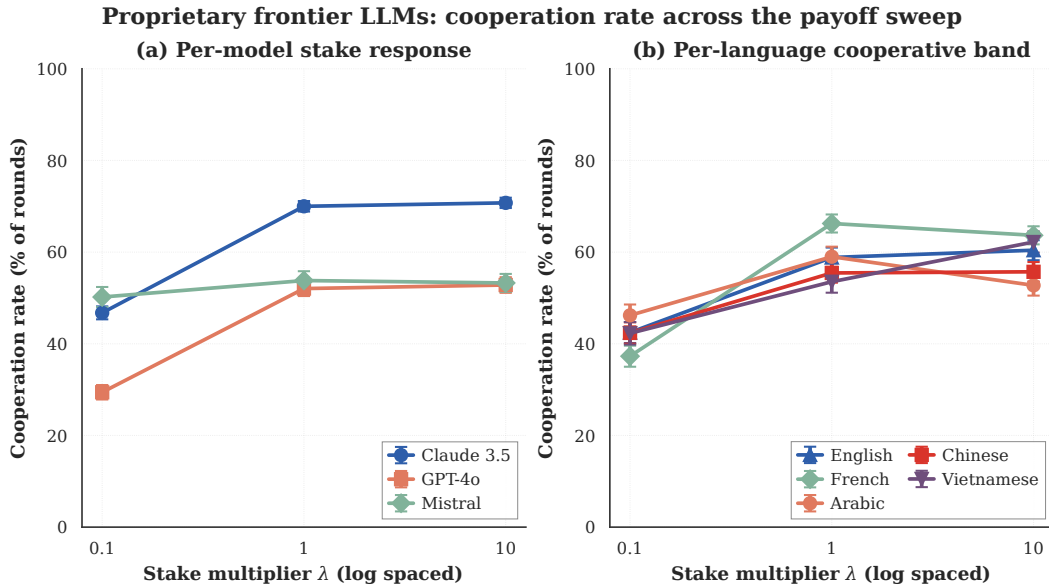


Figure 2: Proprietary frontier LLMs across the payoff sweep. The cooperation rate is the percentage of rounds in which an agent picked Option B (cooperate); higher is more cooperative. **(a)** Per-model view: each model has a distinct stake response – Claude 3.5 climbs steeply from low to moderate stakes and plateaus; GPT-4o shows the largest low-stake defection gap before recovering; Mistral Large is comparatively stake-insensitive. **(b)** Per-language view: French shows the largest stake-driven swing in cooperation, while Vietnamese rises monotonically across the sweep; Arabic and Chinese sit in similar mid-range bands.

The figure tells a short story. First, stake matters: every model and every language shows a higher cooperation rate at $\lambda \in \{1, 10\}$ than at $\lambda = 0.1$. Second, the response is model-specific. Claude lifts roughly twenty-five percentage points of its mass from defection to cooperation as stakes rise, GPT-4o starts from the lowest baseline and shifts the most absolutely, and Mistral Large barely moves at all. Third, the language axis carries comparable signal: French elicits the widest cooperative swing across stakes, while Vietnamese rises steadily into the highest band at $\lambda = 10$. The aggregate picture is consistent with the game-theoretic intuition that low stakes encourage exploratory defection

while higher stakes commit agents to mutually beneficial play [25], but the model-level heterogeneity already hints that there is more going on than the payoff matrix alone explains. The subsections below decompose this picture in terms of inferred strategies and contrast it with the analytical evolutionary baseline.

Figure 3 presents round-by-round choice trajectories. Claude 3.5 Haiku learns to cooperate over time, with attenuated-stake trajectories favouring defection. GPT-4o exhibits the opposite trend, converting to more defective behaviour over time, especially for the higher payoff stakes. Mistral Large shows a different trend, with amplified payoffs correlating with increased defection - consistent with dominant strategy reasoning. A notable spike at Round 2 in Mistral’s trajectories suggests retaliatory or probing behaviour [1].

Our additional analysis (Appendix B.1.1, Figure 17) reveals that varying payoff stakes strongly impact LLM behavioural characteristics [10], particularly their internal variability (the variance of outcomes when the same game scenario is played multiple times).

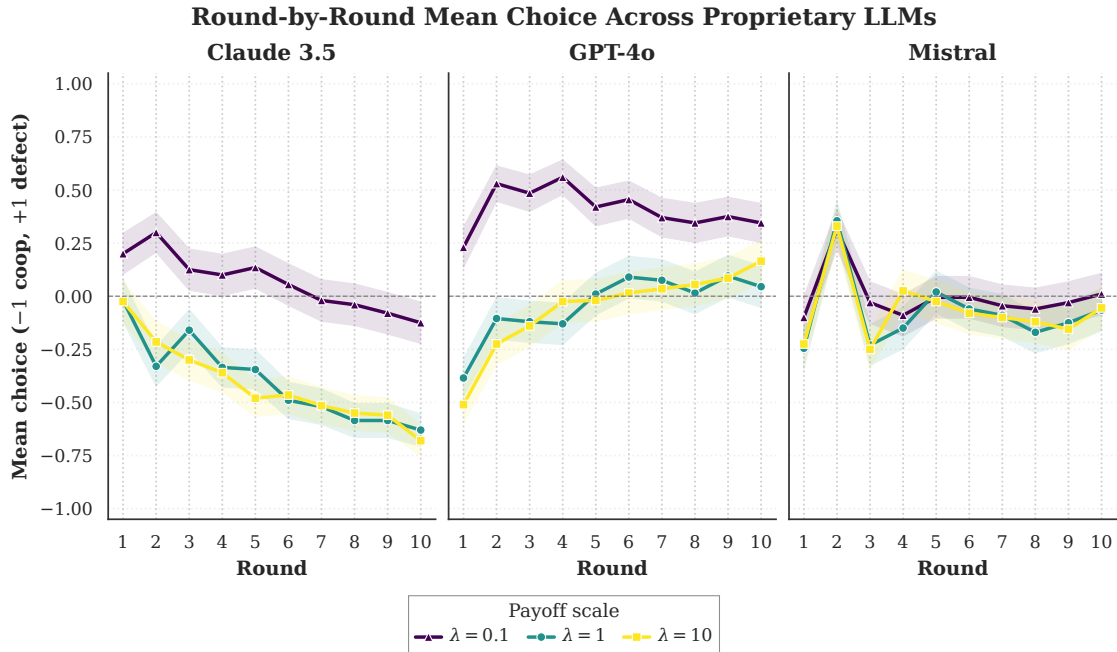


Figure 3: Average trajectory of strategy choices across repeated rounds in all Prisoner’s Dilemma experiments, shown for each proprietary LLM (Claude 3.5 Haiku, GPT-4o, Mistral Large) under different payoff magnitudes. A value of +1 indicates selection of Option A (defection), while -1 corresponds to Option B (cooperation); shaded bands denote standard errors across games. The experiments consider $\lambda \in \{0.1, 1.0, 10.0\}$, representing attenuated, baseline, and amplified penalty scales (viridis colour scale from dark purple to yellow). The three panels make the model-specific stake response visible: Claude 3.5 drifts towards cooperation across the horizon at $\lambda \in \{1, 10\}$, with amplified stakes reaching the most cooperative regime by round 10, while attenuated stakes ($\lambda=0.1$) keep it on the defection side throughout; GPT-4o starts cooperative at $\lambda \in \{1, 10\}$ but drifts steadily towards defection over rounds (consistent with end-game backward-induction reasoning); Mistral Large shows a sharp Round 2 retaliatory spike before settling near the indifference line.

3.2. LLM strategies in repeated games

We apply the intent recognition framework (see Section 2.3) to LLM decision trajectories to examine how their inferred strategic intentions vary with incentive magnitude, linguistic context, and model architecture. Before applying the classifier to unknown LLM trajectories, we validate it against synthetic baselines so we can distinguish genuine strategic shifts from classification artefacts. The LSTM classifier achieves $F1 = 0.984$ on the 4-strategy task at 5% execution noise and remains robust as the strategy space expands, successfully distinguishing behaviourally similar conditional strategies (Tit-for-Tat and Win-Stay-Lose-Shift) [14, 50]. It also outperforms Logistic Regression, Random Forest, and Hidden Markov Model baselines; the full benchmarking is reported in Appendix A.6. Detailed strategy-recognition results on the baseline FAIRGAME corpus (four proprietary models at the default $\lambda=1$ condition) are provided in Appendix B.5, including a per-model supervised-learning breakdown (Appendix B.5.4).

We use a hybrid classification pipeline combining rule-based pattern matching for unambiguous trajectories with LSTM predictions for complex cases. Of the 3,600 agent trajectories (2 agents \times 1,800 games), 2,914 (approximately 81%) achieved classification confidence ≥ 0.9 and were retained for analysis. Details on threshold sensitivity are provided in Appendix A.5; the rationale for selecting $\tau = 0.9$ as the primary cutoff is in Appendix A.4.

Mixed strategies within a trajectory. A single-label assignment risks compressing trajectories that exhibit mid-game strategy switches into the nearest canonical archetype. We probe this in two complementary ways. First, our hybrid pipeline retains *composite* labels of the form “ALLD|TFT” or “ALLC|TFT|WSLS” whenever a trajectory simultaneously satisfies the rule-based definition of more than one canonical strategy. Roughly one in four of the high-confidence trajectories receive such a composite label (see Appendix B.2 for the per-pattern breakdown). Second, we fit a four-state Hidden Markov Model whose hidden states correspond to the four canonical strategies and run Viterbi decoding on every trajectory (Appendix B.3): the fraction of trajectories whose Viterbi path visits more than one hidden state is 20%, of the same order as the rule-based composite-label rate, and the average number of regime switches per trajectory is small (about 0.21 switches per trajectory on average). Crucially, re-aggregating the strategy distribution by redistributing each trajectory’s mass over its visited HMM states preserves the directional stake effect documented in Section 3.2: ALLD share still falls sharply between $\lambda=0.1$ and $\lambda=1$, and ALLC share still rises. We read this as evidence that within-trajectory mixing is real but moderate at the $N=10$ horizon, and that the single-label conclusions are conservative rather than overstated.

Figure 4 shows how strategy distributions shift with payoff scaling. As λ increases from 0.1 to 10, we observe a clear behavioural inversion: unconditional defection (ALLD) sharply declines, effectively halving its prevalence, while conditional cooperation (WSLS) and unconditional cooperation (ALLC) both see marked increases. Tit-for-Tat (TFT) remains relatively stable across conditions. This aligns with standard stake-effect predictions and indicates that LLM agents are not statically aligned: they modulate their strategic commitments with incentive salience, transitioning from opportunistic defection at low stakes toward adaptive reciprocity (WSLS) as the consequences of error become more severe [25, 50].

Strategy Trends by Payoff Scale (Proprietary LLMs)

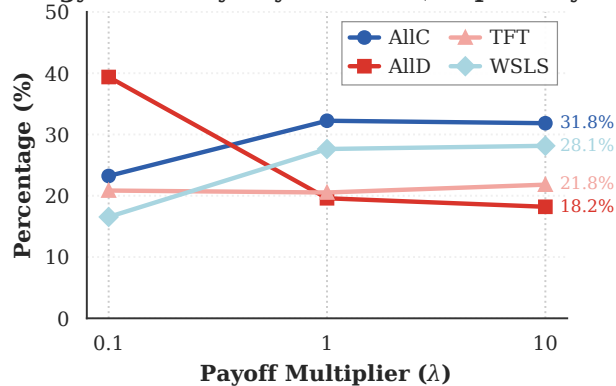


Figure 4: Trends in inferred strategy distributions as a function of the payoff scaling parameter λ . Increasing payoff magnitude systematically shifts LLM behaviour from unconditional defection (ALLD) toward conditional and cooperative strategies (WSLS, ALLC), indicating sensitivity to incentive scale.

Table 1 shows the aggregate and model-specific strategy distributions across all experimental conditions. Three patterns emerge. First, conditional strategies (WSLS and TFT) account for nearly half of all trajectories, almost matching unconditional strategies. This contrasts with game theory, which predicts universal defection in finite-horizon games via backward induction [4, 50]. LLMs instead use heuristics that respond to recent history, similar to bounded rationality in human players [1, 24, 39]. Second, a moderate cooperative bias is evident: ALLC is more frequent than ALLD, consistent across payoff scales, languages, and models. This likely reflects alignment training, such as Reinforcement Learning from Human Feedback (RLHF) and Constitutional AI, optimising for prosocial behaviour [6, 11, 44]. Third, strategic heterogeneity is high: distribution entropy approaches the theoretical maximum,

indicating diverse strategic repertoires. This validates intent classification: aggregate cooperation rates alone would conflate fundamentally different decision rules [14, 24].

Table 1

Overall (aggregate) and model-specific strategy distributions in the payoff-scaled experiments (three models: Claude 3.5 Haiku, Mistral Large and GPT-4o).

Strategy	Overall	Claude	Mistral	GPT-4o
ALLC	29.1%	29.7%	33.7%	23.7%
ALLD	25.9%	19.4%	25.2%	31.7%
TFT	21.1%	25.1%	16.4%	22.8%
WSLS	24.0%	25.8%	24.8%	21.9%

Table 1 also shows model-specific strategy distributions. Claude 3.5 Haiku displays a cooperative strategic profile, with the highest level of overall cooperation (ALLC + WSLS + TFT), which is due to its highest level of conditional cooperation (WSLS + TFT). Mistral Large shows the strongest unconditional cooperation bias, with ALLC being its most frequent strategy, though it retains diversity with ALLD and conditional behaviours. In contrast, GPT-4o exhibits a distinct “hawk” profile, with the highest defection rate. These differences persist across payoff scales and languages [10, 17], suggesting that training procedures and alignment methods imprint distinct strategic priors: some models are inherently “dovish” while others are “hawkish.”

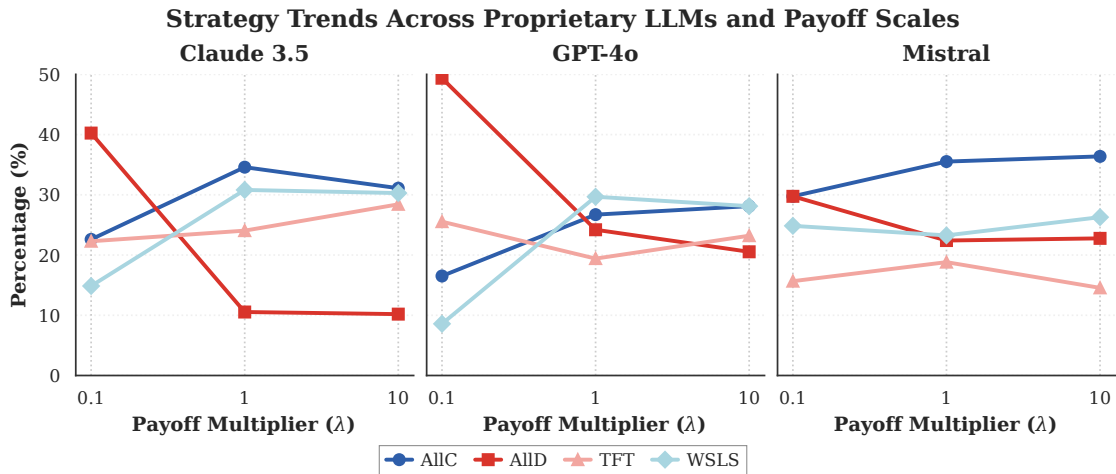


Figure 5: Interaction between payoff scaling and LLM architecture. Each subplot illustrates how inferred strategies evolve with increasing payoff magnitude for a given model, revealing heterogeneous incentive sensitivity across LLMs.

Crucially, Figure 5 shows that these priors interact non-trivially with payoff scaling, revealing *architecture-dependent incentive sensitivity*. Across models, increasing λ systematically shifts behaviour from unstable low-stake patterns toward stable strategies, though the extent of this shift varies by model. Claude and GPT-4o exhibit the highest payoff sensitivity: both models show steep reductions in ALLD prevalence as stakes move from attenuated to baseline levels, effectively abandoning widespread defection when consequences become non-trivial. GPT-4o is particularly responsive, shifting from a strongly defect-heavy regime at low stakes to a more balanced profile at baseline. Mistral Large, by contrast, demonstrates *strategic inertia*: its ALLD rate varies by only a few percentage points across λ values, whereas GPT-4o’s ALLD share roughly halves between attenuated and amplified conditions (from $\approx 49\%$ at $\lambda = 0.1$ down to $\approx 21\%$ at $\lambda = 10$). This matches classical stake-effects where higher stakes amplify commitment to conventions, but highlights a critical nuance for AI governance: some models (like GPT-4o) are essentially rational agents that respond well to penalty tuning, while others (like Mistral) act as committed agents whose behaviour is stubbornly invariant to incentive design [17].

Table 2

Strategy distribution (%) across languages, pooled over all λ values. Arabic and Chinese exhibit the strongest bias toward unconditional strategies (ALLC+ALLD \approx 60%), while English, French, and Vietnamese show more balanced distributions.

Strategy	Arabic	Chinese	Viet.	English	French
ALLC	32%	32%	28%	28%	28%
ALLD	30%	28%	25%	22%	24%
TFT	20%	18%	23%	23%	19%
WSLS	18%	22%	24%	27%	29%

A notable finding is the significant influence of linguistic context on strategic behaviour, an effect we term *linguistic-cultural priming*. Table 2 reveals that languages cluster into distinct strategic archetypes. Arabic and Chinese exhibit a shared bias toward unconditional strategies, with combined ALLC+ALLD around 60%. In contrast, English, French, and Vietnamese show more balanced profiles, with adaptive reciprocity (TFT+WSLS) and unconditional play roughly evenly split. English in particular displays the most uniform distribution across the four strategies, likely reflecting its dominance in training corpora [11]. An aggregated view grouping strategies into unconditional (ALLC + ALLD) vs. conditional (TFT + WSLS) classes is provided in Appendix B.1.3.

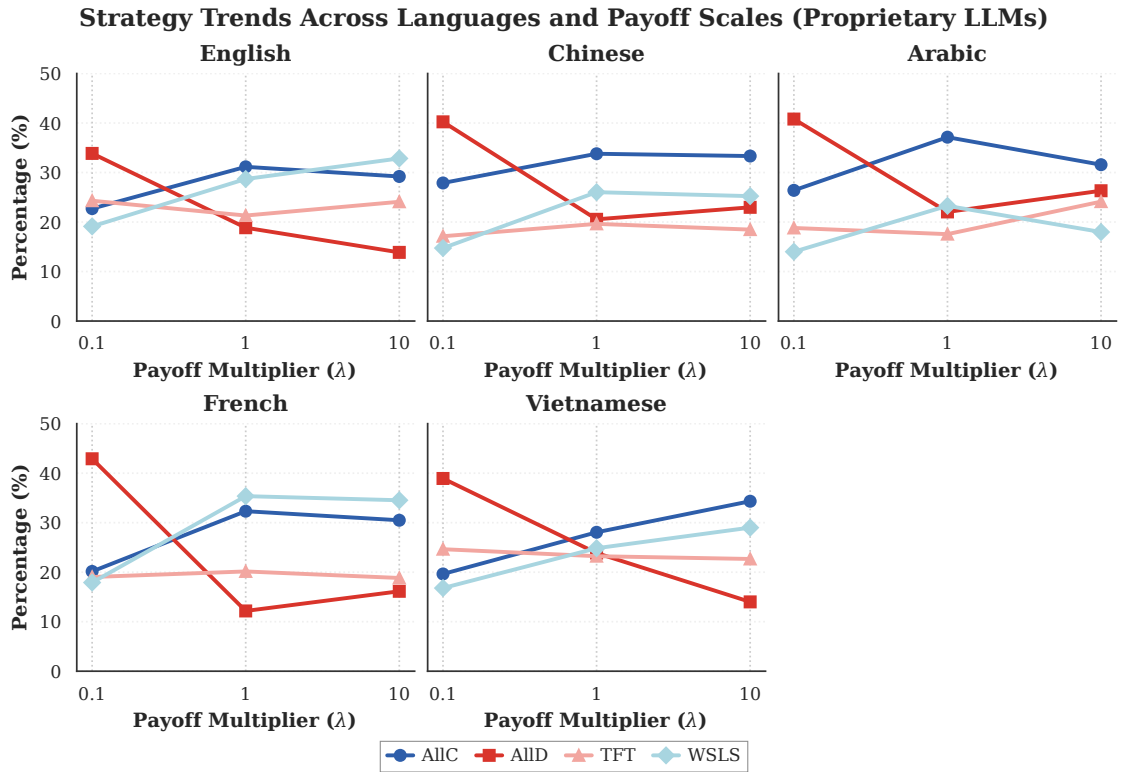


Figure 6: Interaction between payoff scaling and language. Each subplot shows strategy evolution as λ increases from 0.1 to 10. French and Vietnamese show the strongest stake-sensitivity, while Arabic exhibits the most muted response.

Moreover, these linguistic priming effects interact dynamically with incentive magnitude (Figure 6). All five languages start defection-oriented at low stakes but diverge sharply in how rapidly they shift toward cooperation as stakes rise. French and Vietnamese exhibit the strongest stake-sensitivity: French moves from the most defection-heavy profile at attenuated stakes to a WSLS-leading cooperative regime as stakes increase, while Vietnamese sees its cooperative share rise substantially over the same range. Arabic, by contrast, shows the most muted response, suggesting that some culturally-primed biases are more resistant to incentive pressure than others. Notably, at high stakes, English and French converge to nearly identical strategic profiles, suggesting that sufficiently strong incentives

can normalise cross-linguistic variation. This has important implications for AI deployment: while language choice may introduce behavioural biases at low stakes, high-stakes environments may naturally mitigate some of these effects.

3.3. Statistical validation

To move beyond descriptive statistics, we conducted formal hypothesis testing using chi-square tests and factorial ANOVA (Table 3a). The results confirm that stake level significantly affects strategy distributions, and that different LLM architectures exhibit distinct incentive sensitivities. Post-hoc comparisons reveal the largest behavioural differences between attenuated and amplified stake conditions, with small-to-moderate effect sizes consistent with the inherent stochasticity of LLM decision-making [17]. These statistical validations support our core finding: LLM strategic behaviour is systematically, i.e. not merely randomly, influenced by incentive design.

Table 3

Statistical validation summary: (a) hypothesis tests for stake effects, (b) classifier comparison for strategy recognition ($n = 80,640$ test samples, 4-strategy, 5% noise).

(a) Stake effect tests				
Test	Statistic	p	Effect	Sig.
Chi-Square	$\chi^2(6) = 209.25$	< .001	$V = 0.165$	***
1-Way ANOVA	$F(2, 3825) = 48.25$	< .001	$\eta^2 = 0.025$	***
2-Way ANOVA	$F(4, 3823) = 33.66$	< .001	$R^2 = 0.034$	***
(b) Classifier performance				
Model	Acc.	Prec.	Rec.	F1
LSTM	0.984	0.984	0.984	0.984
Random Forest	0.980	0.980	0.980	0.980
State-Factorised	0.956	0.958	0.956	0.956
Neural Network	0.937	0.937	0.937	0.937
HMM	0.777	0.826	0.777	0.780
Logistic Reg.	0.756	0.767	0.756	0.751

Our statistical tests treat trajectories as independent observations; however, the experimental design introduces nested dependencies: 10 repetitions per condition, 10 rounds per game, and 2 agents per game. For the chi-square test, the dependent variable is strategy category (4 levels); for ANOVA, we use a numeric encoding (ALLC= 1, TFT= 2, WSLS= 3, ALLD= 4) aggregated at the trajectory level. Mixed-effects multinomial logistic regression with random intercepts for repetition and game instance would better account for this nested structure and categorical outcomes; we acknowledge this as a methodological limitation. Our fixed-effects approach provides conservative estimates given consistent effect directions across conditions, and the threshold-sensitivity and label-expansion robustness checks reported in Appendices A.5, B.2 and B.3 confirm the stability of our conclusions.

Deep learning models (LSTM, Neural Network) outperform probabilistic models (HMM, State-Factorised) on conditional strategies (TFT: LSTM 0.98 vs HMM 0.74; WSLS: LSTM 0.98 vs HMM 0.73), justifying our methodological choice. The State-Factorised model [17] achieves 0.956 accuracy, providing a strong SFEM-style baseline. While SFEM excels at estimating mixture proportions over long horizons (100+ rounds), our LSTM approach trades mixture flexibility for interpretable point estimates on shorter sequences.

The LSTM achieves near-perfect performance on unconditional strategies (ALLC/ALLD: F1 = 0.99) but exhibits modest confusion between TFT and WSLS under noise, where execution errors can blur characteristic signatures. The Hidden Markov Model (HMM) baseline shows much higher confusion on conditional strategies (F1 \approx 0.74), justifying our LSTM choice. Confidence scores are uncalibrated; threshold sensitivity analysis (Appendix A.5) shows robustness across $\tau \in [0.7, 0.95]$.

3.4. Evolutionary game baseline: stationary strategy distributions under payoff scaling and execution noise

To complement the empirical analysis of LLM strategic preferences with a model-free theoretical benchmark, we computed the long-run frequency of the four canonical policies {ALLC, ALLD, TFT, WSLS} predicted by

evolutionary game theory (EGT) under the same payoff structure introduced in Section 2.2. The purpose of this analysis is twofold: (i) it characterises which strategy mixtures are evolutionarily stable when the only sources of variation are payoff magnitude and stochastic execution, and (ii) it provides a reference distribution against which the LLM-derived frequencies reported above can be directly contrasted. Combining EGT modelling with LLM-based simulations to interpret strategic divergences has recently proved fruitful in studies of AI governance dilemmas [7, 9], and we adopt a similar logic here in the simpler payoff-scaled iterated Prisoner’s Dilemma.

Model. We adopt the standard pairwise-comparison process under the small-mutation limit (SML) [25, 35, 43, 50], in which a finite well-mixed population of size $Z = 100$ evolves through social imitation governed by the Fermi update rule. Small-mutation limit here is a regime where mutations are rare enough that the population spends most of its time in monomorphic states (every individual playing the same strategy) and only occasionally transitions between them; this regime has a clean analytical solution and is the standard reference baseline in finite-population evolutionary game theory. This approximation has proven powerful in providing predictions for human experimental data [49, 56]. Selection intensity is set to $\beta = 0.1$ (weak-to-moderate selection) to suppress numerical overflow at large stakes while preserving the qualitative ordering of strategies. For each pair of resident strategy i and mutant strategy j , the average per-round payoff π_{ij} is computed analytically from a r -round iterated Prisoner’s Dilemma. To ensure that the EGT analysis operates on the same incentive structure as the empirical experiments, we negate the FAIRGAME penalty matrix so that lower-is-better penalties in the empirical game become higher-is-better payoffs in the EGT calculation; this is a strict sign flip and preserves the strategic ordering of the dilemma. Concretely, the FAIRGAME penalties $T_{\text{pen}}=0$, $R_{\text{pen}}=2$, $P_{\text{pen}}=6$, $S_{\text{pen}}=10$ (representing years of imprisonment, so smaller is better) map to EGT payoffs $T=0$, $R=-2$, $P=-6$, $S=-10$ (so larger is better), and the standard Prisoner’s Dilemma ordering $T > R > P > S$ is satisfied in both regimes. The whole matrix is then rescaled by the multiplier λ , identically to the empirical protocol of Section 2.2, so that the EGT and LLM comparisons are anchored to the same per-round incentive magnitudes. The fixation probability of a single j -mutant invading a resident i -population is

$$\rho_{ji} = \left(1 + \sum_{k=1}^{Z-1} \prod_{m=1}^k \frac{T_{ji}^-(m)}{T_{ji}^+(m)} \right)^{-1}, \quad (1)$$

where $T_{ji}^{\pm}(m)$ denote the Fermi-weighted up/down transition rates at composition m [52]. Concatenating these probabilities yields an embedded Markov chain over the monomorphic states whose unique stationary distribution σ encodes the long-run frequency of each strategy in the rare-mutation regime [50]. All quantities are obtained with the analytical pipeline of the open-source EGTtools library [15], with the four canonical policies represented as memory-one strategies parameterised by an implementation-error rate $\varepsilon \in [0, 1]$ that gives the per-round probability of executing the opposite of the intended action.

Figure 7 show the EGT prediction into two complementary panels. The horizon is fixed at $r = 10$ rounds, matching the FAIRGAME experimental protocol [10], and the population size and selection intensity are set as $Z = 100$, $\beta = 0.1$ throughout.

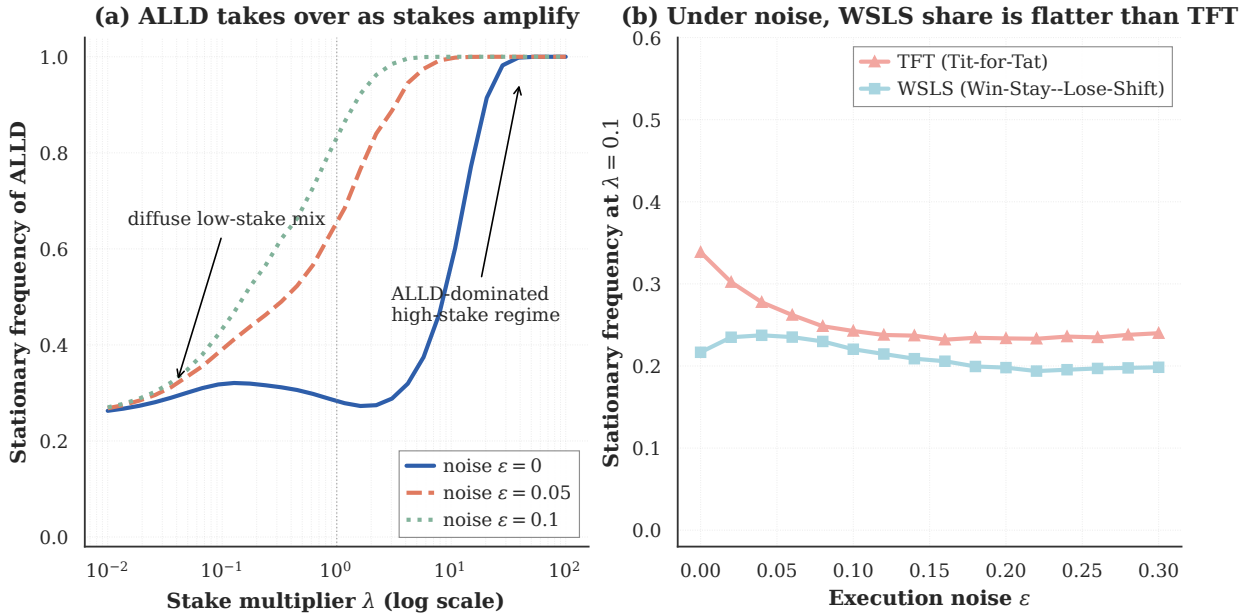
EGT prediction: stake regime \times noise robustness ($r = 10, Z = 100, \beta = 0.1$)


Figure 7: EGT prediction: stake regime \times noise robustness ($r=10, Z=100, \beta=0.1$). (a) Stationary frequency of Always Defect as a function of the stake multiplier λ at three execution-noise levels. The Always-Defect line climbs from a diffuse low-stake mix to near-total dominance as stakes grow, and the three noise lines collapse onto one another in the high-stake regime: noise barely matters once stakes are amplified. (b) At low stakes ($\lambda = 0.1$), holding the stake fixed and varying execution noise ϵ , Tit-for-Tat remains the modal conditional cooperator but its frequency decreases monotonically as noise increases (from $\approx 34\%$ at $\epsilon = 0$ to $\approx 24\%$ at $\epsilon = 0.3$), while the Win-Stay-Lose-Shift frequency is flatter ($\approx 22\text{--}26\%$ across the same range). It is important to note that a single execution error triggers a long sequence of retaliation between Tit-for-Tat players, whereas Win-Stay-Lose-Shift forgives its own mistakes automatically and so resists the noise pressure.

There are two notable observations. First, EGT predicts that high stakes should produce a wall of Always Defect, and the prediction is robust to execution noise: panel (a) shows the three noise curves converging to the same near-unity defection frequency for $\lambda \geq 10$. Second, the noise tolerance of the canonical conditional strategies is markedly asymmetric: panel (b) makes it visible at the stake level where conditional cooperators have any room to live at all. Both observations will feed directly into the comparison with the LLM data in the next subsection. The full per-strategy view at every stake and every noise level is reported in Appendix B.4 as a more detailed reference.

3.5. Comparing EGT predictions and LLM-derived strategies

With the EGT prediction and the LLM data computed under matched conditions, we can finally ask the question that motivates this section: are LLMs playing the game as evolutionary theory expects them to play? Figure 8 answers it visually. At low stakes the two distributions are not so far apart – both lean defection-heavy, both leave some room for conditional cooperators. But as stakes grow the picture splits in two. The EGT bars collapse onto ALLD, as the classical theory says they should; the LLM bars do the opposite, drifting towards Win-Stay-Lose-Shift and unconditional cooperation. The same Prisoner’s Dilemma, played by the same canonical strategies on the same payoff matrix, predicts two qualitatively different worlds depending on *who* is playing – EGT-style agents or LLM agents.

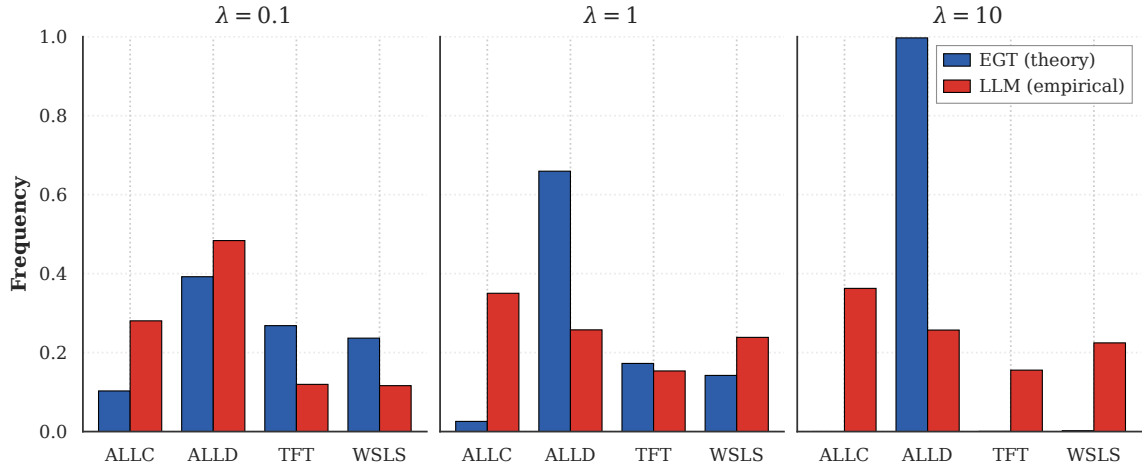
EGT stationary distribution vs. LLM empirical distribution ($\epsilon = 0.05, r = 10, Z = 100, \beta = 0.1$)


Figure 8: EGT stationary distribution (blue) vs. LLM empirical distribution (red) at $\lambda \in \{0.1, 1, 10\}$. EGT computed analytically under the small-mutation limit with the FAIRGAME penalty matrix scaled by λ , $r=10$ rounds, $\epsilon=0.05$ implementation noise, $Z=100$, $\beta=0.1$. LLM frequencies pool high-confidence ($\tau \geq 0.9$) trajectories of Claude 3.5 Haiku, GPT-4o, and Mistral Large across all five languages at the matching λ , with composite (multi-rule) labels expanded into one row per matched canonical strategy so the distribution is consistent with Tables 1–2 and Figure 4. At low stakes ($\lambda=0.1$) the two distributions agree on the ALLD-leading ranking but already disagree on the ALLC mass. As λ rises, EGT concentrates virtually all mass on ALLD ($\approx 97\%$ at $\lambda=10$) while the LLM mix moves in the opposite direction, with ALLC and WSL gaining share and ALLD declining to $\approx 18\%$.

Table 4

Pattern-by-pattern comparison of the EGT stationary distribution and the LLM empirical distribution at $r=10, \epsilon=0.05$. “Evidence” columns refer to figures and tables in this paper; numerical values for the EGT row come from the analytical calculation reported in Section 3.4 and Figure 8, those for the LLM row come from Table 1 and Figure 4.

Pattern	EGT prediction	LLM observation
<i>Agreements</i>		
Stake effect on strategy mix	λ moves mass between conditional cooperators and ALLD	λ shifts mass between ALLD and WSL/ALLC
WSLS share is the most noise-stable conditional strategy	At $\lambda=0.1$, WSLS share holds within $\approx 22\text{--}26\%$ as ϵ ranges over $[0, 0.3]$, while TFT share decays by ≈ 11 percentage points (Fig. 7b)	WSLS share exceeds TFT in all three frontier models at $\lambda \in \{1, 10\}$ (gap of $\approx 2\text{--}12$ pp per model)
Highest behavioural diversity at low stakes	At $\lambda=0.1, \epsilon=0.05$ all four canonical strategies retain non-trivial mass (ALLC $\approx 10\%$, TFT and WSL $\approx 26\%$ each, ALLD $\approx 38\%$)	At $\lambda=0.1$ models maximally diverge in profile (Fig. 5)
<i>Divergences</i>		
Direction of high-stake shift	ALLD concentration grows monotonically, reaching $\approx 97\%$ at $\lambda=10$	ALLD share <i>falls</i> from $\approx 39\%$ at $\lambda=0.1$ to $\approx 18\%$ at $\lambda=10$
ALLC frequency	Near zero at $\lambda \gtrsim 1$ ($< 3\%$)	Persists at $23\text{--}32\%$ for every $\lambda \in \{0.1, 1, 10\}$
Language dependence	Absent: EGT is language-blind	Strong (Table 2)

Table 4 catalogues the agreements and divergences pattern by pattern. A chi-square test confirms what the eye already sees: the two distributions are statistically distinct at every stake we examined, and the gap between them *widens* as λ grows – exactly the opposite of what would happen if LLMs were slowly converging to the rational equilibrium. The two systems are not drifting towards each other; they are pulling apart.

It is worth being clear about where the disagreement actually occurs. The two regimes do not always divert. They both pick up the existence of a stake effect: when consequences become larger, the strategy mix moves, on both sides. They both treat Win-Stay-Lose-Shift as the noise-stable conditional strategy: in the EGT prediction, the WLSL share is markedly flatter than the Tit-for-Tat share as execution noise rises (Fig. 7b), reflecting WLSL’s self-correction from mutual defection [2, 31]; in the LLM data, the WLSL share exceeds the Tit-for-Tat share at $\lambda \in \{1, 10\}$ across our three frontier models. And they both place significant behavioural diversity at the low-stake end – when little is at stake, both real and imagined populations can afford to explore. So far, EGT works as a useful first-order description of LLM strategic behaviour.

The disagreements are concentrated, and they are interpretive. The first is the direction of the high-stake shift. Theory says: when defecting is much more attractive, defection should win. LLMs say: when defecting hurts the partner that much more, defect less. The second is the existence of unconditional cooperation at all. With the same payoff structure, ALLC is strictly dominated and EGT eliminates it; LLMs always maintain a substantial level of ALLC across every stake level we tested. The third is language: the EGT baseline is, by construction, language-blind, while the LLM distribution varies noticeably when the same game is re-prompted in Arabic, Chinese, English, French or Vietnamese.

It is tempting to read this as LLMs getting the game wrong. We think a more useful framing is that LLMs are playing a slightly different game, with three forces layered on top of the payoff matrix. The first is alignment training: RLHF and Constitutional AI [6, 44] reward prosocial completions, and that reward becomes most visible when penalties are strong, which is exactly the amplified-stake regime. The second is the human source of LLM training data: people in real repeated games tend to escalate cooperation, not defection, as the consequences of error grow [33, 34], and LLMs appear to have absorbed that pattern. The third is the prompt itself, which carries cultural connotations that evolutionary theory has no way of representing – and so the EGT baseline cannot, by design, see the language effects we observe. In this way, the EGT baseline becomes useful precisely because it is naive: it tells us what the strategy mix would look like if payoffs and execution noise were the only forces in play, so that any systematic gap between EGT and LLM measures the contribution of the LLM-specific layers on top. This is the same logic that Balabanova et al. [7] arrived at in a governance setting – and the consistency between their finding and ours is, in our view, the strongest single argument for treating EGT not as a competing predictor of LLM behaviour but as a normative reference against which LLM-specific biases can be diagnosed.

3.6. Open-weight small LLMs

A natural objection to everything reported so far is that proprietary frontier models share a narrow slice of the wider language-model landscape: they are large, aligned by similar Reinforcement Learning from Human Feedback (RLHF) pipelines, and trained on overlapping corpora. If our story is really about how language models behave as strategic agents – and not about a specific generation of GPT and Claude – the same patterns should hold when we step outside that slice. We therefore re-ran the payoff-scaled protocol on three open-weight small models that can be served locally on a single accelerator: Qwen3 8B [48], Gemma-3 12B [20], and Llama-3.1 8B [36]. The design follows Section 2.2 exactly, with two extensions. First, the game horizon is extended from ten to thirty rounds, to ensure robustness of the previous consideration of ten rounds which might be short for slow conditional strategies to surface can be put to rest. Second, the set of stakes is widened to six multipliers, $\lambda \in \{0.01, 0.1, 1, 10, 100, 1000\}$, spanning five orders of magnitude. Both extensions are deliberate: the wider range lets us look for any breakdown of the directional stake effect at extreme stakes, and the longer horizon lets us see whether late-game dynamics differ from the proprietary models. To match the extended game horizon, the LSTM component of the hybrid classifier was retrained on 30-round synthetic trajectories using the same architecture described in Section 2.3. A complementary classification on the first ten rounds is reported in Appendix B.6.2 as a horizon-robustness check; it yields the same qualitative picture. In total, the open-weight replication covers 3 models \times 5 languages \times 6 λ values \times 4 personality pairings \times 10 repetitions = 3,600 games, yielding 216,000 agent decisions (each game produces 60 decisions across $N=30$ rounds for 2 agents).

Open-weight small LLMs: cooperation rate across the full stake sweep

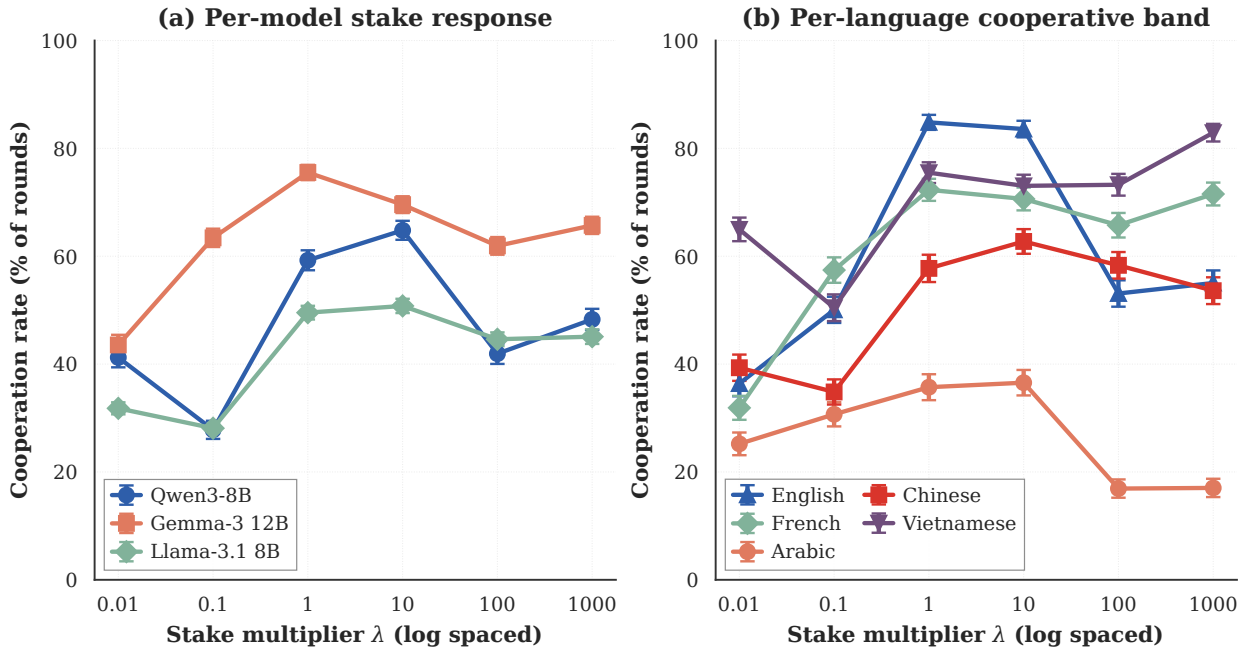


Figure 9: Open-weight small LLMs across the full stake sweep. Both panels show the cooperation rate – the percentage of rounds in which an agent picked Option B (cooperate) – as a function of the stake multiplier λ on a log-spaced axis. Error bars are standard errors over games. **(a)** Per-model view: each model has a different stake response. Gemma-3 12B occupies the highest cooperative band at almost every stake; Qwen3 8B traces a clear U-shape with its valley at the low-stake end; Llama-3.1 8B sits in the defection-leaning band, with a milder hump in the middle of the sweep. **(b)** Per-language view: each language occupies its own cooperative band. Vietnamese sits in the upper cooperative band across the sweep; Arabic the lowest; English shows the widest swing, peaking near $\lambda = 1$ and falling back at the very largest stakes.

There are three key observations, see Figure 9. The directional stake effect of the main analysis is reproduced: cooperation rises as λ grows out of the lowest cells. But it is not monotonic. At the very largest stakes, $\lambda \in \{100, 1000\}$, cooperation no longer keeps rising and in some cases drifts back down; the strongest version of this U-shape is Qwen3, whose cooperation rate climbs from roughly a quarter to roughly two-thirds and then partially relaxes. The middle of the sweep – $\lambda \in \{1, 10\}$ – is where cooperation is highest, suggesting that there is a particular range in stake magnitude that an EGT would not predict at all. And the model identities matter: Gemma-3 inhabits the cooperative band across every stake, Llama-3.1 stays in the defection-leaning band, and Qwen3 occupies a context-sensitive middle zone. The proprietary observations about personality (cooperative pairings do better than selfish ones) and language (each model has its own cooperative language) remains with the open-weight corpus. Further detailed per-(language, pairing) penalty breakdown is provided in Appendix B.6.1.

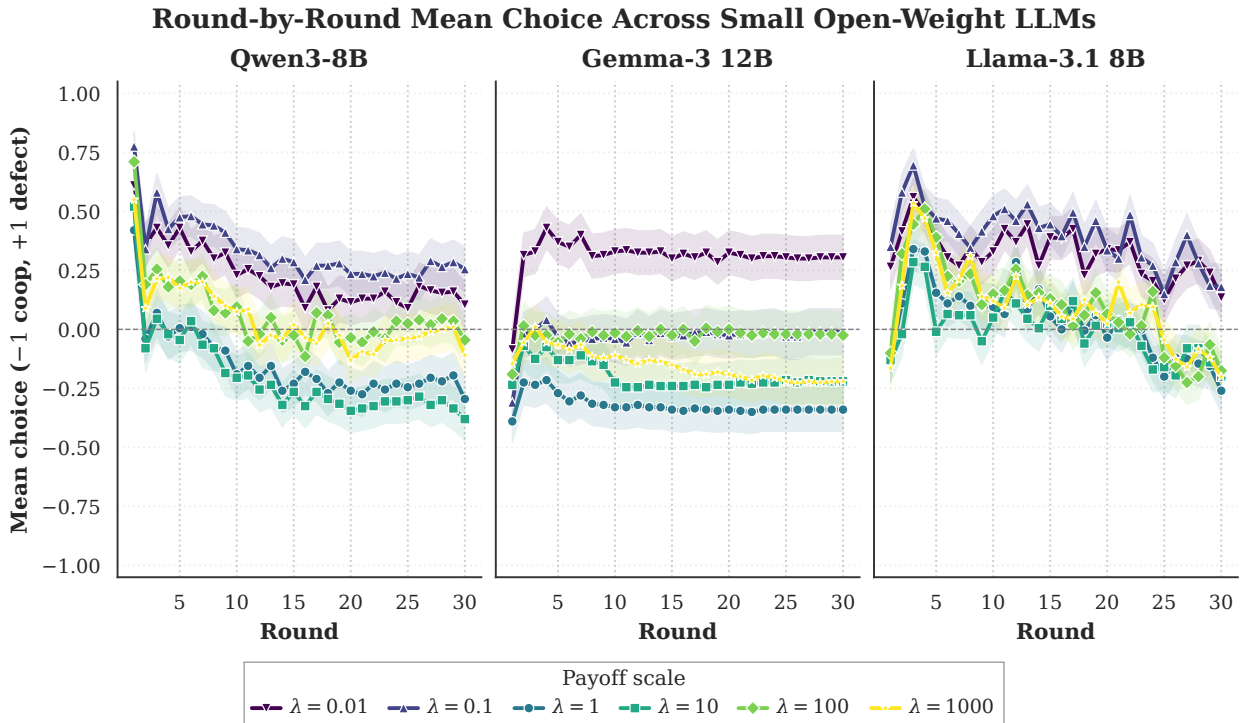


Figure 10: Round-by-round mean choice trajectories for the three open-weight LLMs over the full $N=30$ rounds. The encoding (+1: defection; -1: cooperation) follows Figure 3. All three models shift towards cooperation as λ rises. Qwen3 8B remains highly defective throughout at $\lambda=0.1$ (mean choice $\approx +0.3$ to $+0.8$), while at $\lambda=\{1, 10\}$ it drifts steadily from a defection-leaning round 1 towards a cooperative regime by round 30 with no end-game defection spike. Gemma-3 12B is essentially stationary across rounds in every λ condition. Llama-3.1 8B exhibits the largest stake-induced level shift in the mean-choice (± 1) encoding: defection-heavy throughout at $\lambda=0.1$, mixed early oscillation at $\lambda=\{1, 10\}$ that gradually settles into a mildly cooperative regime by the final rounds.

The round-by-round trajectories (Figure 10) show the same story from a different angle. Gemma-3 commits to a policy in the first two rounds and then sticks to it, as a fixed-strategy player rather than a learner. Qwen3 keeps adjusting throughout the game, never fully settling, which fits its U-shaped stake response: a model that is constantly recalibrating to context is also a model that can be pushed in either direction by where the stake falls. Llama-3.1 keeps changing its behaviour round-by-round but remains highly defective on average. None of the three open-weight models shows the late-game defection spike that backward induction would predict and that we observe in the proprietary trajectories: their cooperation, where it appears, persists to the last round. The most likely interpretation is that smaller models have shorter effective planning horizons and do not count down to the end of the game.

Table 5

Aggregate and per-model strategy distribution (%) for the open-weight small LLMs ($N=30$ rounds, analysed with the hybrid intention-recognition pipeline of Section 2.3, with the LSTM component retrained on 30-round synthetic trajectories to match the extended game horizon). Shares are normalised over canonical strategy assignments at the $\tau=0.9$ confidence threshold; composite labels (e.g. “TFT|WSLS” when both strategies are matched) are expanded into one row per matched strategy before normalising.

Strategy	Overall	Qwen3 8B	Gemma-3 12B	Llama-3.1 8B
ALLC	20.74	21.19	21.60	17.46
ALLD	18.00	27.35	12.59	16.41
TFT	41.98	35.55	40.85	57.00
WSLS	19.28	15.91	24.96	9.13

Table 5 shows the aggregate and per-model strategy distributions pooled over the extended stake range. Zooming in on which strategies underlie that cooperation reveals model-specific behavioural fingerprints (Figure 11). Gemma-3 stays balanced across the four canonical strategies at every stake, never letting any single mode dominate – a kind of strategic generalist. Llama-3.1 does the opposite: at moderate stakes it collapses onto Tit-for-Tat, becoming the most committed reciprocator in the corpus, while at the extremes it tips back toward Always Defect. Qwen3 sits in between, with a U-shaped Always Defect curve whose valley is at the moderate stakes where the model is most cooperative. None of these patterns is what EGT would predict: the theory expects every model to walk uphill toward Always Defect as stakes grow, and only Llama-3.1 even partially follows that script.

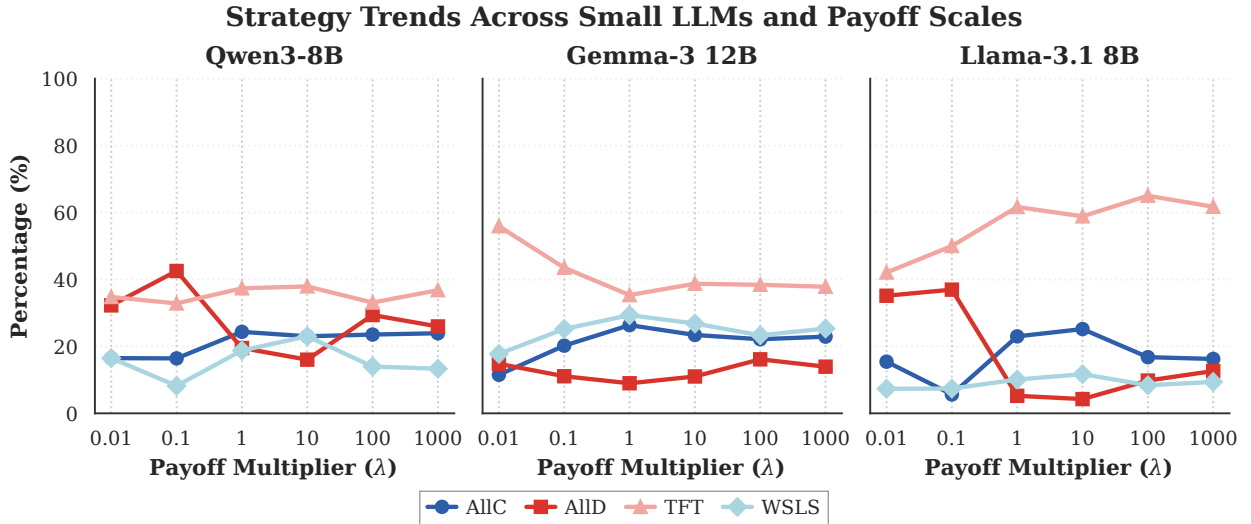


Figure 11: Inferred strategy share for each open-weight LLM as a function of the payoff scaling parameter λ , normalised over canonical strategy assignments. The model-level interaction is heterogeneous: Gemma-3 12B remains comparatively low in ALLD (9–16%) and balanced across the other three strategies at every stake; Llama-3.1 8B carries an elevated ALLD share at $\lambda \in \{0.01, 0.1\}$ but converges onto a strongly TFT-dominated profile (TFT $\approx 60\%$) from $\lambda = 1$ onward; and Qwen3 8B traces a U-shaped ALLD response, peaking at low stakes (42.5% at $\lambda = 0.1$) and again at very high stakes (26–29% at $\lambda \in \{100, 1000\}$), with a more balanced conditional mix in between.

Table 6

Strategy distribution (%) across languages for the open-weight small LLMs (pooled over models and λ , normalised over canonical strategy assignments). Arabic is the most defection-heavy language, while Vietnamese has the largest TFT and WSLS shares and French has the highest ALLC share.

Strategy	Arabic	Chinese	Viet.	English	French
ALLC	14.78	20.54	22.15	21.46	24.85
ALLD	33.92	17.73	9.61	14.54	14.17
TFT	41.41	40.74	44.57	42.76	40.27
WSLS	9.89	20.99	23.67	21.24	20.71

The language story (Table 6 and Figure 12) shows a similar trend: each prompt language sits in a different cooperative band, and the rank ordering survives the entire stake range. Vietnamese is the most reciprocity-oriented language, carrying the highest pooled Tit-for-Tat and Win-Stay-Lose-Shift shares and the lowest pooled Always Defect; the same ordering survives at the per-multiplier level for most, though not all, stakes. Arabic is the consistently defection-leaning language and the only one in which Win-Stay-Lose-Shift is essentially absent. English is the most stake-sensitive language, with cooperation rising sharply between the low and middle stakes and then easing back at the very largest stakes – the U-shape we saw at the model level reappears here, sharpest on the English line of Figure 9b. French and Chinese fall between these extremes. The takeaway is that stake magnitude and prompt language interact:

stake reshapes *how much* cooperation a model produces, but the linguistic priors set *which kind* of cooperation – direct copy (Tit-for-Tat), self-correcting reciprocity (Win-Stay–Lose-Shift), or unconditional cooperation – the model reaches for to produce it.

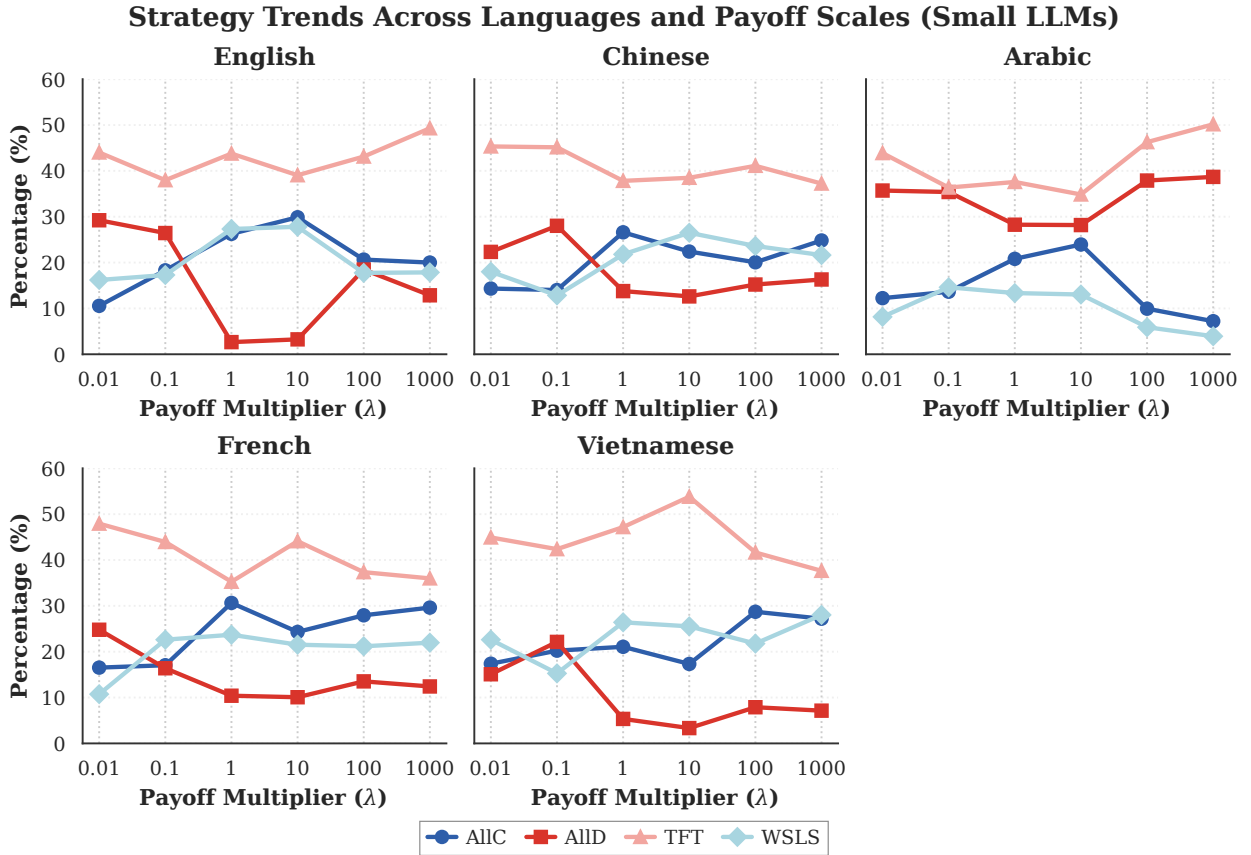


Figure 12: Strategy share by language and payoff scaling for the open-weight LLMs (normalised over canonical strategy assignments). Arabic maintains the most defection-heavy profile across stakes; English exhibits the largest stake-driven retreat from ALLD (from 26–29% at $\lambda \in \{0.01, 0.1\}$ down to under 4% at $\lambda \in \{1, 10\}$). Vietnamese carries the highest TFT share at most stakes and a consistently elevated WSLS share; French carries the highest ALLC share at moderate stakes ($\lambda = 1$) and at the largest stake ($\lambda = 1000$), with Vietnamese or English topping the ALLC ranking at the intermediate stakes ($\lambda \in \{10, 100\}$).

The corresponding radar charts and three-way (language \times model \times game-stake) visualisations are reported in Appendix B.1.1 and Appendix B.1.2 respectively, alongside the matched figures for the proprietary models so the two corpora can be inspected side by side. Additional robustness checks for the open-weight corpus – including confidence-threshold sensitivity (Appendix B.6.3) – are collected in Appendix B.6.

Putting the two corpora side by side in Figure 13 provides a clear summary of what does and does not transfer between the proprietary and open-weight settings. What *transfers* is the directional stake effect: in both groups, raising λ out of the lowest cells pulls mass away from unconditional defection and toward conditional cooperation – exactly the pattern that, in Section 3.5, we argued is the most striking departure from the evolutionary baseline. The fact that this same signature reappears in a corpus of much smaller, openly released models that were not aligned by the same teams is, we argue, the strongest evidence we have that the divergence between evolutionary game theory and language models is a property of language models as a class, not an artefact of a particular vendor or generation. What does *not* transfer is the texture of the cooperation. The proprietary corpus partitions itself roughly evenly across the four canonical strategies, while the open-weight corpus leans approximately two-to-one on Tit-for-Tat over Win-Stay–Lose-Shift (TFT 41%, WSLS 21%; ratio $\approx 1.96:1$), which suggests that the smaller models implement reciprocity by

copying the opponent’s last action rather than by reading the joint outcome of the round. Whether this is a scale effect, a training-data effect, or a representational limitation of smaller models is an open question we leave for future work.

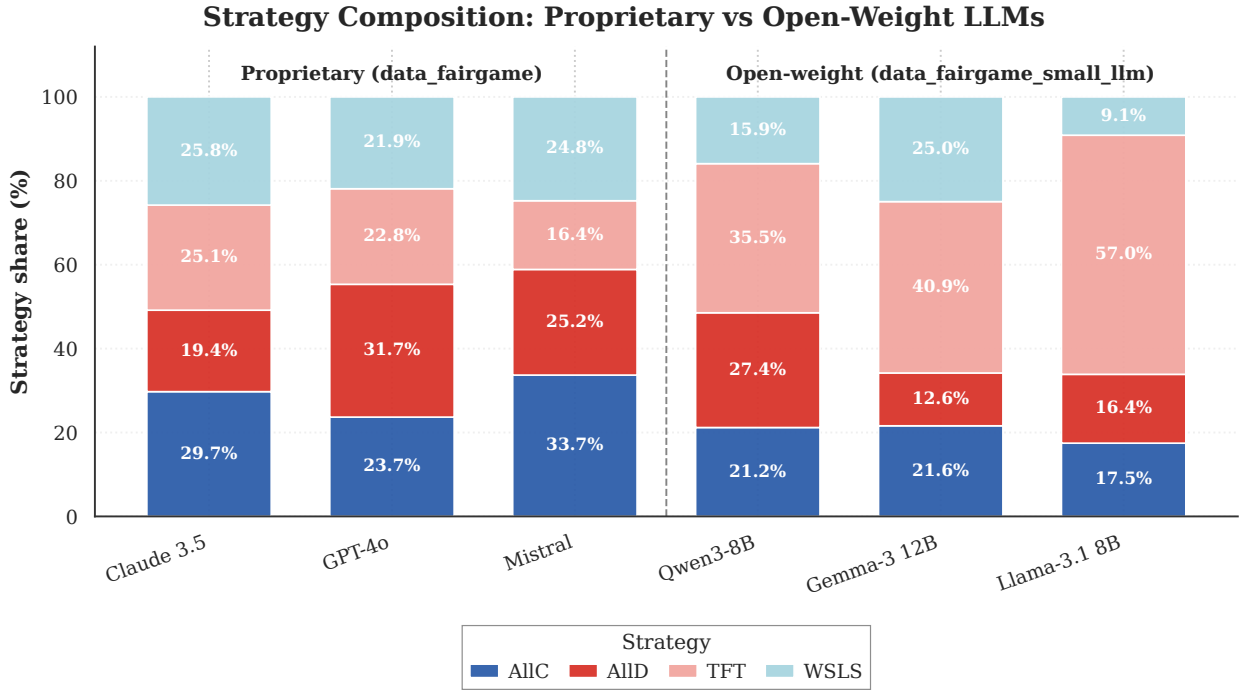


Figure 13: Strategy distribution: proprietary frontier models vs. open-weight small models. Pooled high-confidence strategy frequencies of the three proprietary models (Claude 3.5 Haiku, GPT-4o, Mistral Large at $N=10$ rounds) and the three open-weight small models (Qwen3 8B, Gemma-3 12B, Llama-3.1 8B at $N=30$ rounds) under the matched payoff-scaling design ($\lambda \in \{0.1, 1, 10\}$). The proprietary corpus partitions roughly evenly across the four canonical strategies (ALLC 29%, ALLD 26%, WSLS 24%, TFT 21%), whereas the open-weight corpus is TFT-dominated (TFT 41%, ALLC 22%, WSLS 21%, ALLD 16%). The directional stake effect is reproduced in both corpora; the open-weight corpus shows an approximately 2:1 ratio of TFT to WSLS, consistent with a history-matching rather than outcome-conditioning style of reciprocity.

A chi-square test on the high-confidence trajectories confirms that the dependence of strategy on stake is statistically significant in this corpus too, across all six stake values (p -values well below 10^{-20} for every model and below 10^{-49} for the pooled corpus; full per-model statistics in Appendix B.6.4). The Cramér’s V effect sizes range from about 0.10 for Gemma-3 (consistent with its stake-stable behaviour) to about 0.22 for Llama-3.1 (consistent with its sharper between-stake collapse onto Tit-for-Tat at moderate λ).

Read together, these results give us three things. First, the headline pattern of the paper – LLMs becoming more cooperative as stakes grow, in direct contradiction to the EGT prediction – is not a frontier-model artefact. Second, the language and personality levers we identified for the proprietary models are at least as informative at the open-weight scale, and perhaps more so, since open-weight models have a wider behavioural range. Third, model identity still matters: each of the three open-weight models has a distinct strategic personality, from Gemma-3’s balanced four-way mix, through Qwen3’s U-shaped sensitivity to extreme payoffs, to Llama-3.1’s committed Tit-for-Tat, and that personality coexists with the cross-cutting stake and language effects rather than overriding them. The diagnostic framework – game-theoretic benchmarking, EGT baseline, supervised intent classification – therefore generalises, and the cooperation biases it surfaces are not idiosyncratic to a small set of models. The conclusion is not driven by the longer horizon used for the open-weight runs either: an explicit check truncating each open-weight trajectory to its first ten rounds and re-classifying it (Appendix B.6.2) preserves both the agreement rate and the directional stake effect.

4. Discussion

We have shown that LLMs are sensitive to two control variables that are rarely considered as control variables at all – the size of the stakes of the interaction in place and the language of the prompt – and that this sensitivity has a structure we can recover. Higher stakes pull LLMs towards reciprocal and cooperative behaviours; the language of the conversation among LLM agents pushes them towards either committed or adaptive strategies in patterns that correlate, loosely, with the cultural connotations of those languages in training data. Both effects are statistically confirmed in Section 3.3. Neither lever is exotic, and neither is currently part of standard safety evaluations. Both shift behaviour by amounts that, in our data, rival the differences between model families.

Our central empirical claim – that simply *raising the stakes* of the underlying dilemma tilts LLMs towards cooperation – is complementary to a parallel line of work that asks how external *mechanisms* change LLM cooperation. CoopEval [54] benchmarks contracts and mediation as cooperation-sustaining mechanisms; MoralSim [5] shows that moral framing modulates LLM cooperation in dilemmas where ethics and payoffs collide; cheap-talk pre-play communication has recently been shown to stabilise LLM strategic reasoning [38]. The reading we propose is that stake magnitude joins this list of cooperation levers: an intervention on the *numerical* structure of the game, which sits alongside the linguistic and institutional interventions emphasised by these neighbouring lines of work. Our findings thereby provide empirically grounded strategy profiles for LLM agents that can be directly integrated into models of evolutionary dynamics in hybrid human–AI populations, where artificial and human players co-evolve under shared incentive structures [22].

The EGT comparison provides important and highly informative insights. Read literally, the comparison is a falsification result: evolutionary theory predicts that high stakes should produce result in high levels of defection, and LLMs produce the opposite. Read more usefully, it is a measurement: the gap between the EGT prediction and the LLM data is a quantitative signature of everything LLMs bring to the table that an evolutionary model does not – alignment training, the cooperative bias of the human corpus, the cultural baggage of natural language. The fact that an independent EGT–LLM analysis of AI governance [7, 9] arrives at structurally similar mismatches – LLM agents deviating from the rational equilibrium in the prosocial direction – gives us some confidence that this is a real signal and not particular to our pipeline. Treating EGT as the null model and the LLM–EGT gap as the thing to be explained provides a productive way to read future studies of LLMs in strategic settings.

The open-weight replication shows the robustness of our findings for the frontier models (GPT and Claude). The same direction of stake effect, the same kind of language sensitivity, the same model-specific personalities all reappear at the 8–12B scale. The composition of the cooperation – whether it is implemented through Tit-for-Tat or Win-Stay-Lose-Shift, whether it survives to the end of the game or collapses into late defection – does change with scale, which is itself an interesting object for future work. But the high-level conclusion that LLMs are, for now, more cooperative than the underlying game-theoretic structure justifies appears to be robust across the scales we examined.

There are notable important implications for AI governance. Safety audits that run in English under fixed payoff conditions test a single point on a much larger behavioural surface. A model that is cooperative in English at moderate stakes can become measurably less cooperative in another language at low stakes, and the gap is not negligible. We would argue for adding two simple stress dimensions to existing evaluation suites – a sweep over the stake of the underlying interaction, and a parallel run in the prompt’s non-English variants – and for anchoring the resulting measurements to an EGT baseline whenever the strategic structure permits it. This is what makes the difference between describing what an LLM *does* and understanding what it is responding *to*.

We conclude by noting several important caveats regarding the scope and limitations of our analysis. First, our intent classifier is restricted to four canonical strategies, so more complex strategy classes such as Zero-Determinant play [26, 47], mixed policies, extortionate strategies is mapped into the nearest canonical type. The hybrid rule pipeline does retain a *composite* label whenever a trajectory satisfies more than one canonical rule, and roughly one in four high-confidence trajectories falls in that composite category (Appendix B.2); re-attributing these trajectories under a uniform-mass tie-breaking rule shifts the aggregate frequencies by only a few percentage points and does not affect any qualitative conclusion. Nevertheless, the underlying single-label assumption constitutes a substantive modelling choice, and a mixture or segmentation model along the lines of SFEM [17] or the probabilistic estimators of [42] would be a natural next step.

Second, the ten-round known-horizon setting we use with the proprietary models is conducive to backward-induction defection in the final rounds, and although the thirty-round runs with the open-weight models argue that

this is not what drives the main stake effect, the question of whether the high-stake cooperation pattern survives an *indefinite*-horizon condition is open and worth a follow-up.

Third, our decoding settings follow each provider’s recommended defaults: GPT-4o and Claude run at temperature 1.0 while Mistral Large runs at 0.3, and this difference cannot be cleanly separated from architectural effects in our data; a controlled ablation that fixes temperature and top- p across models would tighten the causal story.

Fourth, the EGT baseline maps LLM stochasticity onto a symmetric per-action flip probability ϵ , which is a clean theoretical object but a coarse abstraction of LLM variability: cognitive heuristics, prompt sensitivity, and end-game reasoning are not well captured by symmetric flips. Accordingly, the EGT calibration we report should be treated as a reference distribution rather than a fitted model. An empirical estimation of an effective ϵ from LLM self-play against deterministic opponents would tighten this link, and we leave it for future work.

Fifth, our statistical tests treat trajectories as independent observations even though the design has nested dependencies (two agents per game, ten or thirty rounds per game, ten repetitions per condition); mixed-effects multinomial models with random intercepts for game and repetition would be more rigorous, and the effect sizes we report should be read as approximations. Finally, we have not benchmarked against human data on the same payoff matrix; that comparison, on which a separate literature exists [33, 34], is the next natural step.

In summary, language and incentives are not implementation details but fundamental control variables, and the strategies that LLMs exhibit in repeated interactions are most appropriately understood as the joint outcome of these control variables, the underlying game structure, and the model-specific layers inferred from discrepancies between empirical behaviour and an evolutionary baseline.

Declaration of competing interest

The authors declare that they have no known competing financial interests or personal relationships that could have appeared to influence the work reported in this paper.

Acknowledgements

T.A.H. is supported by EPSRC (grant EP/Y00857X/1) and also acknowledges travel support from the HCMUT-VNUHCM (Adjunct Professorship scheme HCMUT-VNUHCM).

A. Supplement to Methodology

A.1. LLM configuration

Table 7 summarises the configuration of LLM backends used in our experiments. Following the FAIRGAME protocol [10], we adopt each provider’s recommended default settings to reflect realistic deployment conditions.

Table 7

LLM backend configurations. Temperature and sampling parameters follow each provider’s recommended defaults. While this introduces potential variability confounds in cross-model comparisons, it reflects realistic deployment conditions where practitioners use models “out of the box.”

Model	Provider	Temperature	Top_p
GPT-4o	OpenAI	1.0	1.0
Claude 3.5 Haiku	Anthropic	1.0	1.0
Mistral Large	Mistral AI	0.3	1.0

A.2. Payoff scaling examples

For illustration, the scaled payoff matrices under the three experimental conditions are shown below. When $\lambda = 0.1$ (attenuated stakes), the row player’s payoff matrix becomes:

	Option A	Option B
Option A	(0.6, 0.6)	(0, 1.0)
Option B	(1.0, 0)	(0.2, 0.2)

When $\lambda = 10.0$ (amplified stakes), it becomes:

	Option A	Option B
Option A	(60, 60)	(0, 100)
Option B	(100, 0)	(20, 20)

The ordering $T < R < P < S$ is preserved in all cases, ensuring the strategic structure of the Prisoner’s Dilemma remains unchanged while only the magnitude of incentives varies.

A.3. Rule-based strategy assignment

To complement the LSTM-based strategy predictions and address cases where behavioural patterns exhibit characteristics of multiple canonical strategies, we apply deterministic rule-based algorithms to identify all potential strategy labels consistent with observed action sequences. These rules encode the defining characteristics of each strategy as logical conditions on the agent’s action trajectory $\mathbf{a} = (a_1, a_2, \dots, a_T)$ and the opponent’s history $\mathbf{o} = (o_1, o_2, \dots, o_T)$.

Always Cooperate (ALLC). The agent cooperates in all rounds regardless of opponent behaviour:

$$\text{ALLC} \equiv \forall t \in \{1, \dots, N\} : a_t = C$$

Always Defect (ALLD). The agent defects in all rounds regardless of opponent behaviour:

$$\text{ALLD} \equiv \forall t \in \{1, \dots, N\} : a_t = D$$

Tit-for-Tat (TFT). The agent cooperates in round 1, then copies the opponent’s previous action. To accommodate execution errors, we tolerate up to ϵ_{noise} deviations from pure TFT logic:

$$\text{TFT} \equiv (a_1 = C) \wedge \left(\sum_{t=2}^N \mathbb{1}[a_t \neq o_{t-1}] \leq \epsilon_{\text{noise}} \cdot (N - 1) \right)$$

where $\mathbb{1}[\cdot]$ is the indicator function and $\epsilon_{\text{noise}} = 0.1$ in our implementation.

Win-Stay-Lose-Shift (WSLS). The agent repeats its previous action if the outcome was a Reward (R , mutual cooperation) or Temptation (T , successful defection), and switches otherwise. The initial action can be either C or D . Similarly, we tolerate up to ϵ_{noise} deviations:

$$\text{Let } \hat{a}_t = \begin{cases} a_{t-1} & \text{if } (a_{t-1}, o_{t-1}) \in \{(C, C), (D, C)\} \\ \neg a_{t-1} & \text{if } (a_{t-1}, o_{t-1}) \in \{(C, D), (D, D)\} \end{cases}$$

$$\text{WSLS} \equiv \sum_{t=2}^N \mathbb{1}[a_t \neq \hat{a}_t] \leq \epsilon_{\text{noise}} \cdot (N - 1)$$

These rules are applied sequentially to each trajectory. A trajectory may receive multiple labels if it satisfies conditions for overlapping strategies (e.g., a short sequence of all-cooperate satisfies both ALLC and TFT, and a short sequence of all-defect satisfies both ALLD and TFT). The hybrid pipeline combines these rule-based assignments with LSTM predictions: high-confidence LSTM outputs ($\tau \geq 0.9$) are retained, while ambiguous cases ($\tau < 0.9$) are supplemented with rule-based labels when applicable. Whenever the rule set fires on more than one canonical strategy, we retain all matched labels as a *composite* label of the form “ALLD|TFT” or “ALLC|TFT|WSLS” rather than collapsing to a single “priority” strategy; in our corpus, approximately 24.4% of high-confidence proprietary trajectories receive such a composite label (see Appendix B.2 for the per-pattern breakdown). For aggregate statistics, every composite label is then expanded into one row per matched strategy before normalising, so a trajectory whose rule set fires on ALLC, TFT and WSLS contributes equal mass to each of the three. This approach ensures both coverage (via rules for unambiguous patterns) and robustness (via LSTM for noisy, complex cases).

A.4. High-confidence filtering rationale

We employed a selective filtering approach to ensure the reliability of our LLM behavioural strategy analysis. Specifically, we focused our analysis on game instances where the predicted strategy labels for both agents exhibited prediction probabilities exceeding 0.9 (90% confidence threshold). The decision to use high-confidence predictions is grounded in several key considerations:

- **Pattern alignment with theoretical strategies:** Samples with prediction probabilities above 0.9 indicate that the observed behavioural sequences of LLMs closely align with the canonical patterns defined by the four classical strategies (ALLD, ALLC, WSLS, and TFT).
- **Signal-to-noise separation:** While the probabilities are not absolute (not reaching 1.0), this is expected and attributable to inherent noise in LLM decision-making processes.
- **Statistical reliability:** By focusing on high-confidence predictions, we minimise the risk of misclassification and ensure that our strategy distribution analysis reflects genuine behavioural patterns.

A.5. Threshold sensitivity analysis

To validate our choice of confidence threshold $\tau = 0.9$, we conducted a systematic sensitivity analysis across $\tau \in [0.3, 0.95]$ for 3-, 4-, and 5-strategy classification models. Figure 14 illustrates how retention rate, average confidence, number of predictions retained, and strategy diversity vary as a function of threshold value.

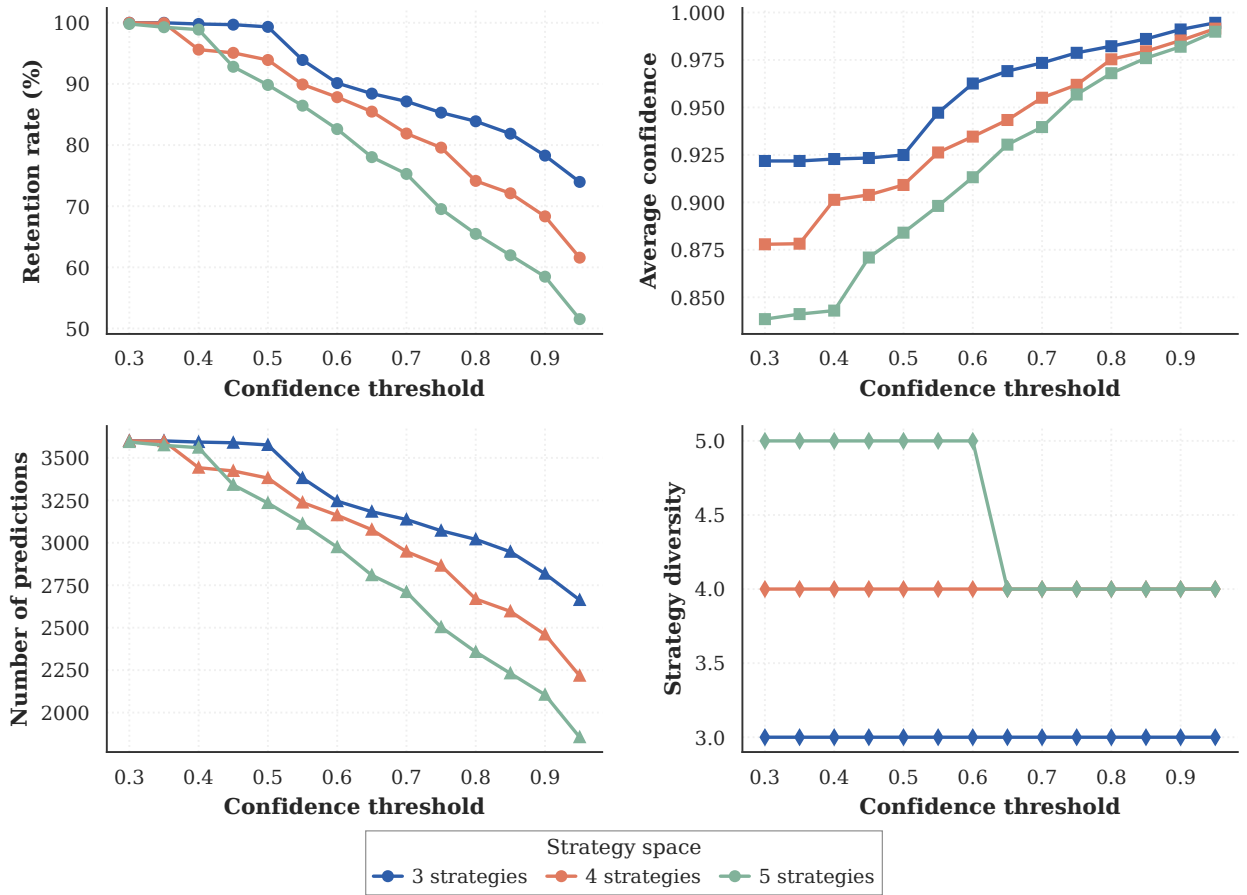
Threshold Sensitivity – Comprehensive View


Figure 14: Comprehensive threshold sensitivity analysis for payoff-scaled experiments. Top row: retention rate and average confidence vs. threshold. Bottom row: number of predictions retained and strategy diversity. The 4-strategy model at $\tau = 0.9$ provides optimal balance between coverage and reliability (avg. confidence 0.985). Note that 68.3% is the LSTM-only retention at this threshold; the full hybrid pipeline (Section 2.3) reaches $\approx 81\%$ by supplementing low-confidence LSTM cases with rule-based labels.

Table 8 summarises key metrics at $\tau = 0.9$.

Table 8

Threshold sensitivity at $\tau = 0.9$ across strategy models.

Metric	3-Strat	4-Strat	5-Strat
Retention Rate	78.3%	68.3%	58.5%
Avg. Confidence	0.991	0.985	0.982
Diversity	3	4	4

Key findings: (1) Retention rate decreases as strategy space expands, reflecting greater behavioural complexity; (2) Average confidence remains > 0.97 at $\tau = 0.9$ across all models; (3) Lowering to $\tau = 0.7$ would increase retention to 75–87% but reduce average confidence to 0.94–0.97. Our choice of $\tau = 0.9$ prioritises classification reliability while maintaining sufficient coverage for statistical analysis.

Table 9 reports the inferred strategy distribution on the proprietary corpus across $\tau \in \{0.7, 0.8, 0.9, 0.95\}$, computed under the same composite-label expansion as Table 1 so the two tables are directly comparable. The

qualitative picture is essentially invariant: retention drops from 90.8% to 75.5% as the threshold rises, but the per-strategy frequencies move by less than one percentage point anywhere in the table, and the rank ordering of the four strategies is preserved at every threshold. This is direct evidence that the substantive conclusions of Section 3.2 are not artefacts of the specific confidence cutoff chosen.

Table 9

Threshold sweep for the proprietary corpus: retention rate and inferred strategy frequencies across $\tau \in \{0.7, 0.8, 0.9, 0.95\}$, computed with composite-label expansion (Appendix B.2). The $\tau \geq 0.9$ row matches the overall row of Table 1. The distribution is essentially stationary in τ , and the rank ordering of the four strategies is preserved.

τ	Retention (%)	ALLC (%)	ALLD (%)	TFT (%)	WSLS (%)
0.70	90.83	28.25	25.93	21.53	24.28
0.80	86.22	28.67	26.18	21.23	23.92
0.90	80.94	29.05	25.86	21.06	24.03
0.95	75.50	28.83	25.22	21.48	24.48

A.6. Classifier robustness across noise and strategy space

This appendix benchmarks the LSTM intent recogniser used throughout the paper. Two complementary views are reported: (i) how the LSTM scales as the strategy space grows from 3 to 5 canonical strategies (Figure 15), and (ii) how the LSTM compares against Logistic Regression and Random Forest baselines under execution noise (Figure 16).

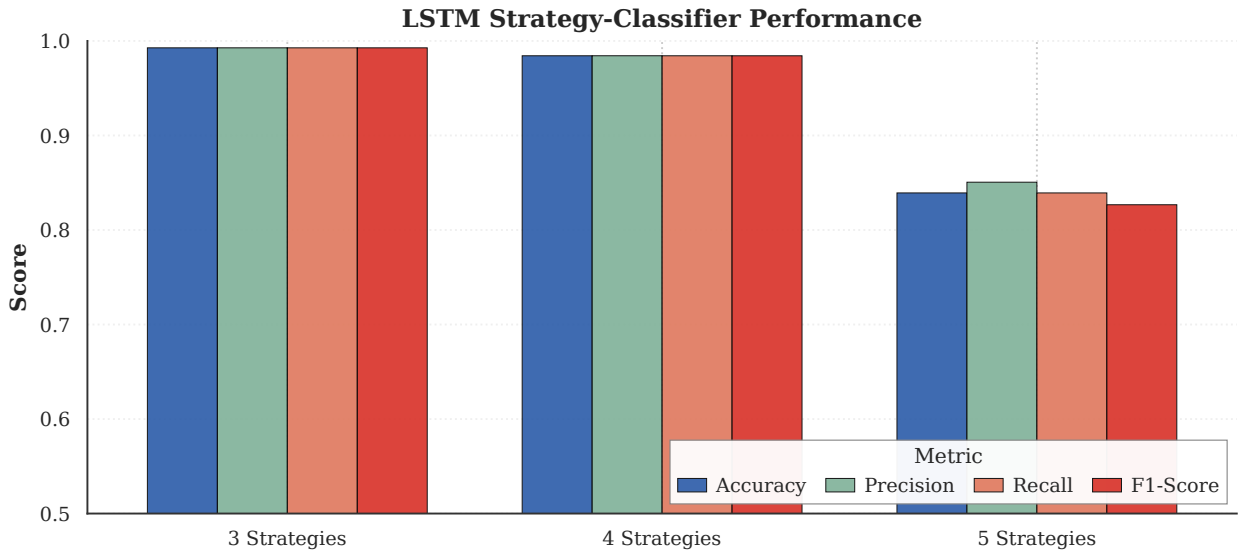


Figure 15: LSTM intent recogniser performance across strategy-space sizes. Accuracy, precision, recall and F1-score on synthetic trajectories with 5% execution noise. F1 ranges from 0.984 (4-strategy task) to 0.83 (5-strategy task); all main-text analyses use the 4-strategy classifier (F1 = 0.984).

Figure 15 confirms the LSTM maintains robust performance even as the strategy space expands, successfully distinguishing between behaviourally similar conditional strategies (Tit-for-Tat and Win-Stay-Lose-Shift) within our analysed set of four canonical strategies. The recurrent architecture’s ability to filter execution noise common in LLM outputs makes it particularly well-suited for this task [14, 24].

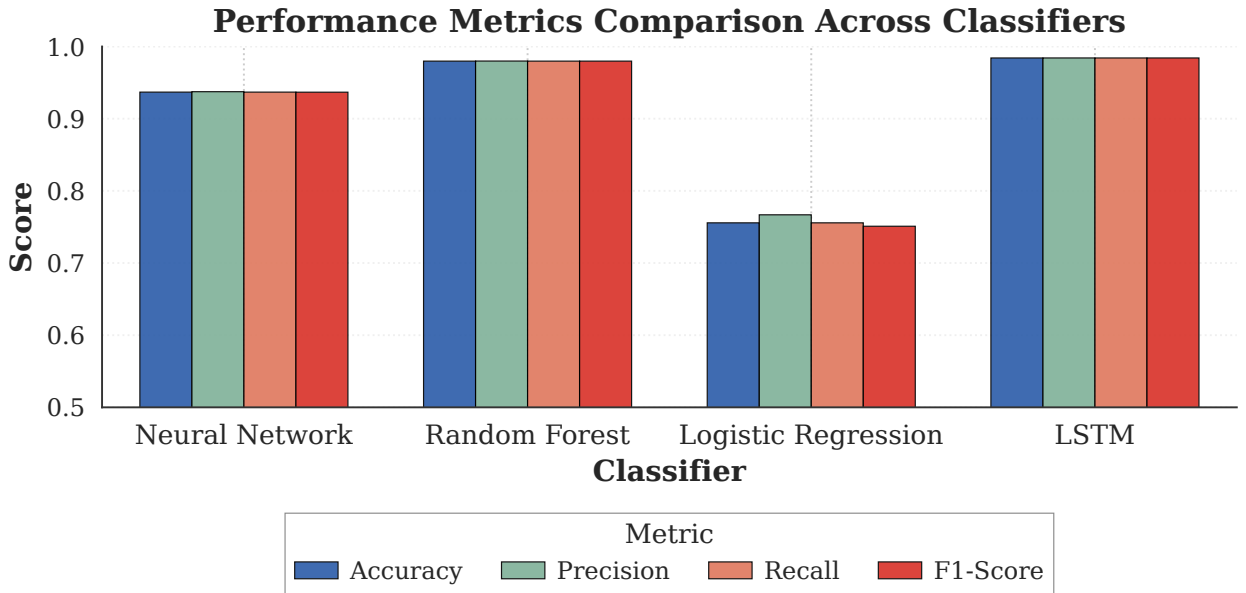


Figure 16: Model robustness to noise. Comparison of accuracy and F1-score between Logistic Regression, Random Forest, and LSTM on no-noise and noise 0.05 datasets. The LSTM demonstrates superior resilience to execution noise.

We also evaluated the robustness of different classifier architectures against execution noise, which simulates the stochasticity and potential “hallucinations” of LLMs. As shown in Figure 16, while Logistic Regression (LR) and Random Forest (RF) models achieved near-perfect accuracy (greater than 0.9) on clean data, their performance degraded when introduced to 5% execution noise. In contrast, the Long Short-Term Memory (LSTM) network maintained the highest accuracy (~ 94%). This superiority stems from the LSTM’s recurrent architecture, which allows it to learn the sequential “context” of a strategy, effectively “forgiving” random deviations to identify the core behavioural pattern.

B. Supplement to Results

B.1. Payoff-scaled experiments: additional analyses

This section provides supplementary analyses for the payoff-scaled Prisoner’s Dilemma experiments (see main paper).

B.1.1. Per-stake behavioural metrics

To visualise the behavioural profiles of different LLM architectures across payoff scaling conditions, we present radar charts comparing normalised metrics for each stake/multiplier setting. Figure 17 displays four key behavioural dimensions - internal variability (IV), cross-language inconsistency (CI), variability over round (VR), and sensitivity-to-payoff (SP) - normalised within each multiplier condition to enable direct cross-model comparison.

Per-multiplier Behavioral Metrics (normalized within λ)

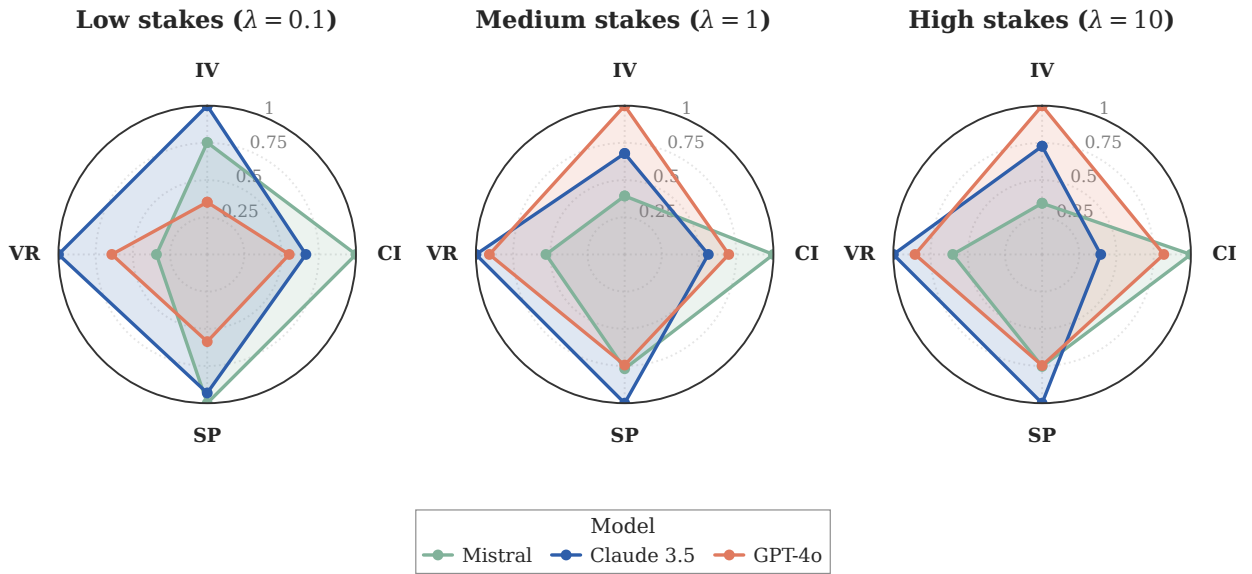


Figure 17: Per-multiplier behavioural metrics. We report four standardised metrics defined in the FAIRGAME framework [10]: (1) **Internal Variability (IV)**, which quantifies the stochasticity of an agent’s behaviour by measuring the variance of outcomes across identical experimental repetitions; (2) **Cross-Language Inconsistency (CI)**, which measures the standard deviation of agent performance across the five tested languages to indicate sensitivity to linguistic framing; (3) **Variability over Round (VR)**, which captures the volatility of decision-making and strategy changes throughout the 10-round game horizon; and (4) **Sensitivity-to-Payoff (SP)**, which reflects the magnitude of behavioural adaptation in response to varying incentive stakes. Radar charts compare Mistral Large (green), Claude 3.5 Haiku (orange), and GPT-4o (blue) across three payoff scales ($\lambda \in \{0.1, 1, 10\}$). Compared to the baseline payoff ($\lambda = 1$), similar scores are observed for the higher stake payoff ($\lambda = 10$). At low stakes ($\lambda = 0.1$), models exhibit divergent scores. Overall, internal variability (IV) is most affected by varying the payoff stake.

Key observations include: (1) at attenuated stakes ($\lambda = 0.1$), the three models display maximally divergent behavioural signatures, with Claude 3.5 Haiku exhibiting elevated variation rate while GPT-4o shows stronger cooperation index; (2) at baseline stakes ($\lambda = 1$), models begin to converge toward more balanced profiles; (3) at amplified stakes ($\lambda = 10$), all models shift toward higher CI and SP values, suggesting that increased consequences promote both cooperative behaviour and strategic consistency. These radar visualisations complement the line plots in the main paper by providing a holistic view of multi-dimensional behavioural shifts.

Per-multiplier behavioural metrics (small LLMs, normalised within λ)

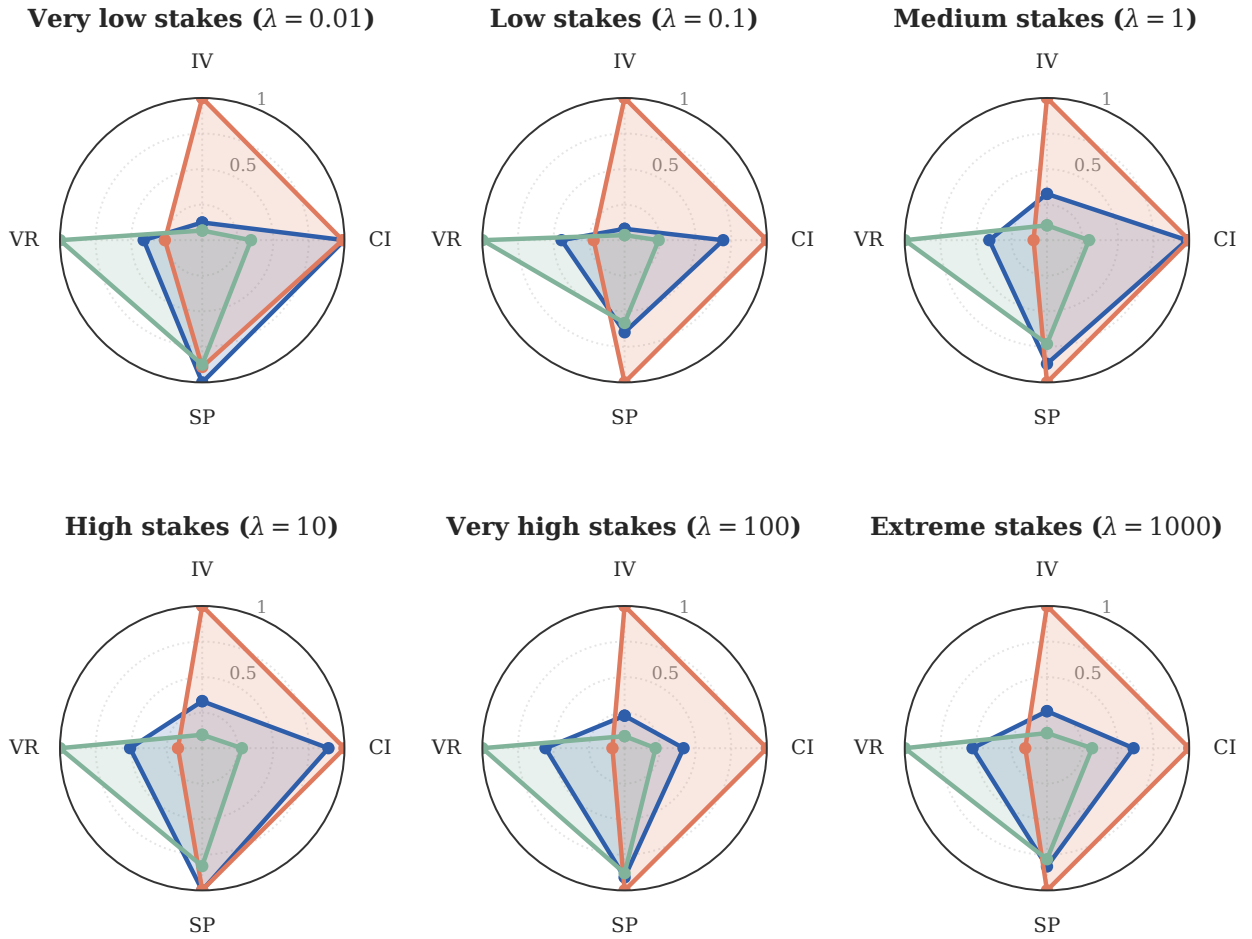


Figure 18: Per-multiplier behavioural metrics for the open-weight small LLMs. The four standardised FAIRGAME metrics (IV, CI, SP, VR) – defined identically to Figure 17 and computed directly from the round-by-round OptionA/OptionB decisions in Dataset/data_fairgame_small_llm/ – are reported for Qwen3 8B (blue), Gemma-3 12B (orange), and Llama-3.1 8B (green) across all six payoff scales covered by the small-LLM corpus ($\lambda \in \{0.01, 0.1, 1, 10, 100, 1000\}$). Each panel is normalised within λ (divide-by-max across the three models), matching the proprietary radar so that the two figures can be read side by side. Two regime patterns are visible across the full sweep: Gemma-3 12B exhibits the largest internal variability (IV) at every λ , indicating the most stochasticity across identical repetitions, while Llama-3.1 8B exhibits the largest within-trace volatility (VR), indicating frequent round-by-round switching. Cross-language inconsistency (CI) peaks at very high stakes ($\lambda \geq 100$) and, like the proprietary panel, the sensitivity-to-payoff proxy (SP) compresses toward the upper end as stakes grow.

B.1.2. Multidimensional behavioural comparison

The visualisation in Figure 19 provides a synoptic view of how the three cardinal dimensions of our study - payoff magnitude, linguistic context, and model architecture - interact to shape agent behaviour. By synthesising these factors, we observe that strategic behaviour is not driven by a single determinant but emerges from their complex interplay. Notably, the variance attributable to linguistic context (visualised across the language axes) often rivals or even exceeds the variance between distinct model architectures, challenging the notion of fixed, immutable “model personalities.”

Furthermore, the impact of payoff scaling is shown to be non-uniform; while amplified stakes generally compress behavioural diversity towards cooperation, the specific trajectory of this shift is heavily modulated by the language in which the game is framed. This suggests that alignment interventions must account for this multidimensional sensitivity, as a model aligned for safety in English may exhibit divergent, risk-seeking behaviours when prompted in other languages or under different incentive structures.

Multi-dimensional Comparison of Behavioral Characteristics Across Models

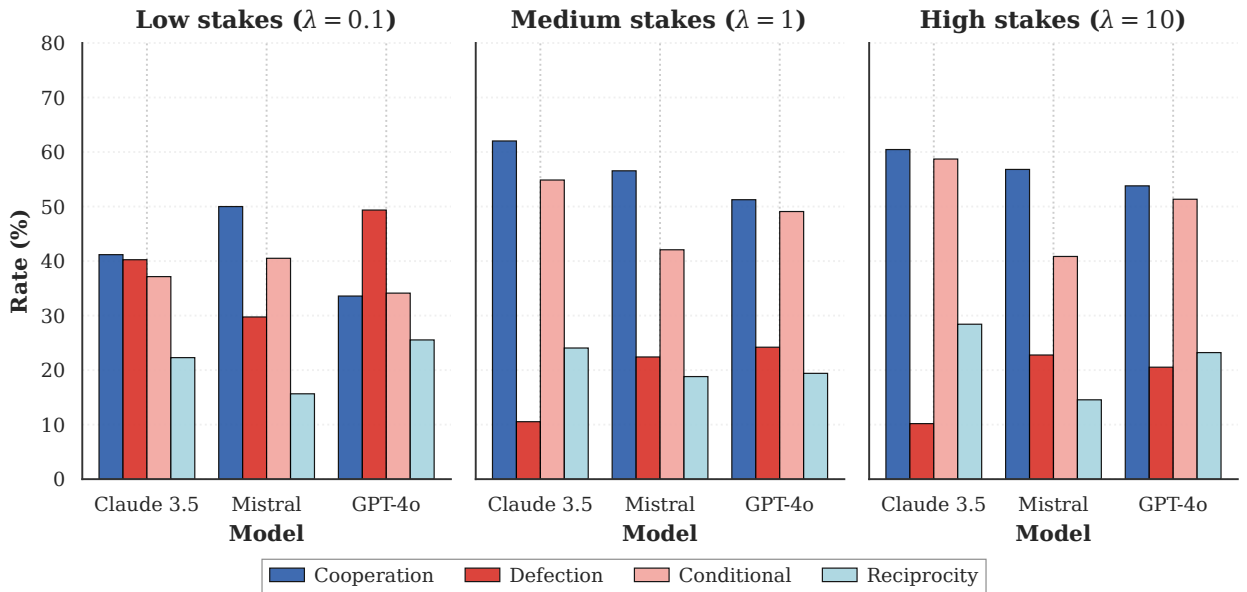


Figure 19: Multidimensional comparison of LLM behavioural strategies across payoff scales, languages, and model architectures. The figure synthesises incentive sensitivity, linguistic priming, and architectural bias, illustrating that language effects can rival or exceed model-level differences.

Multi-dimensional Comparison of Behavioral Characteristics Across Models

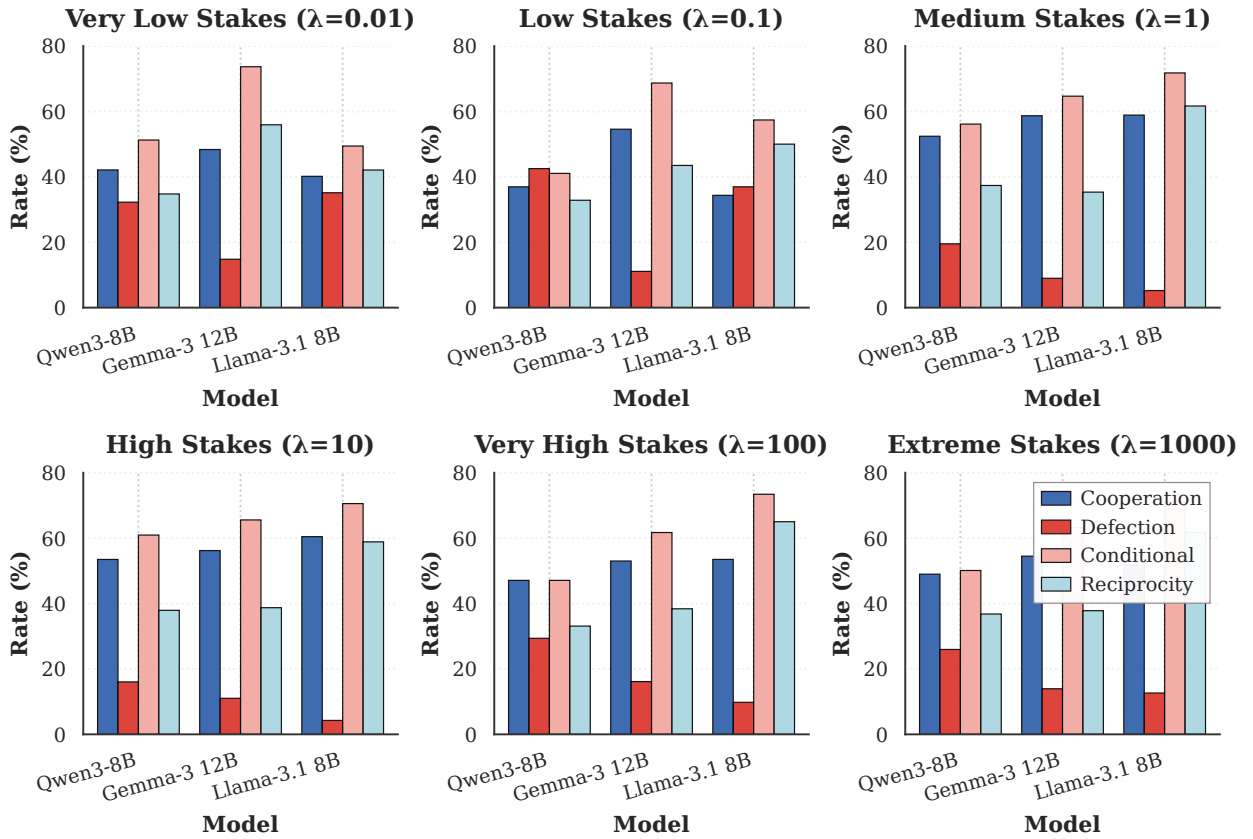


Figure 20: Multidimensional behavioural comparison of the open-weight small LLMs across payoff scales, languages, and model architectures. The figure synthesises incentive sensitivity, linguistic priming, and architectural bias in the same way as Figure 19 for the proprietary models. Language effects again rival or exceed model-level differences, and the impact of payoff scaling is heavily modulated by the prompt language.

B.1.3. Unconditional vs. conditional strategy aggregation

To provide a higher-level view of strategic tendencies across linguistic contexts, we aggregate the four canonical strategies into two categories: *unconditional* (ALLC + ALLD) and *conditional* (TFT + WSLs). This aggregation reveals whether agents commit to fixed policies regardless of opponent behaviour, or adapt their strategies based on interaction history.

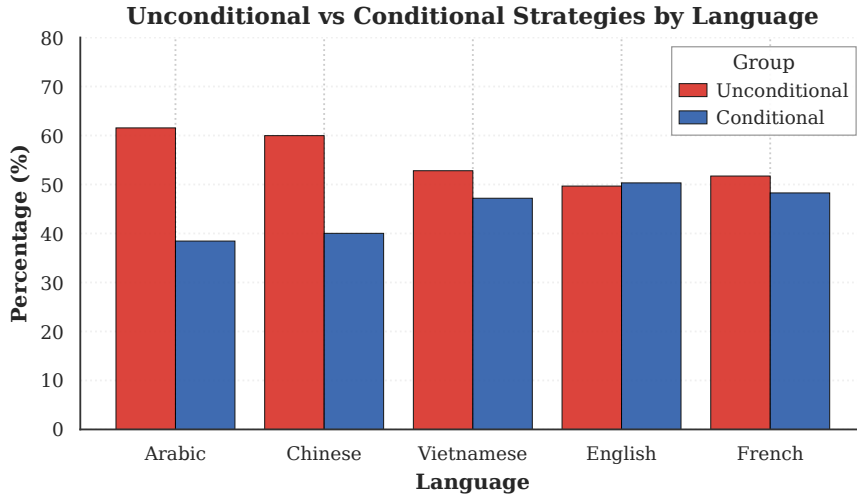


Figure 21: Unconditional versus conditional strategy aggregation across languages (payoff-scaled experiments). Arabic and Chinese exhibit the highest unconditional rates, while English, French, and Vietnamese sit near a balanced split. This aggregated view complements the language strategy distribution table in the main paper.

As shown in Figure 21, Arabic and Chinese prompts elicit predominantly unconditional behaviour, while English, French, and Vietnamese sit close to a balanced split between unconditional and conditional play. This pattern corroborates the fine-grained analysis in the main paper, suggesting that linguistic context systematically modulates the degree to which LLM agents engage in adaptive versus committed strategic behaviour.

B.1.4. Per-condition penalty breakdown (proprietary models)

The compact cooperation-rate view in the main text (Figure 2) is summarised from a much richer underlying dataset that crosses three stake regimes, five languages, three personality pairings and three proprietary models. Figure 22 reports the per-cell mean penalties at the three stake regimes shown in the main text. Two design choices are visible immediately: agents incur lower penalties at higher stakes when measured in normalised units (because the cooperative outcome is rewarded relatively more), and personality framing shifts behaviour systematically (cooperative–cooperative pairings consistently incur lower penalties than selfish–selfish ones). The Arabic prompts elicit elevated defection in cooperative pairings – the “Arabic anomaly” that also appears in the open-weight corpus.

Payoff scaling shapes cooperation in LLM agents across languages

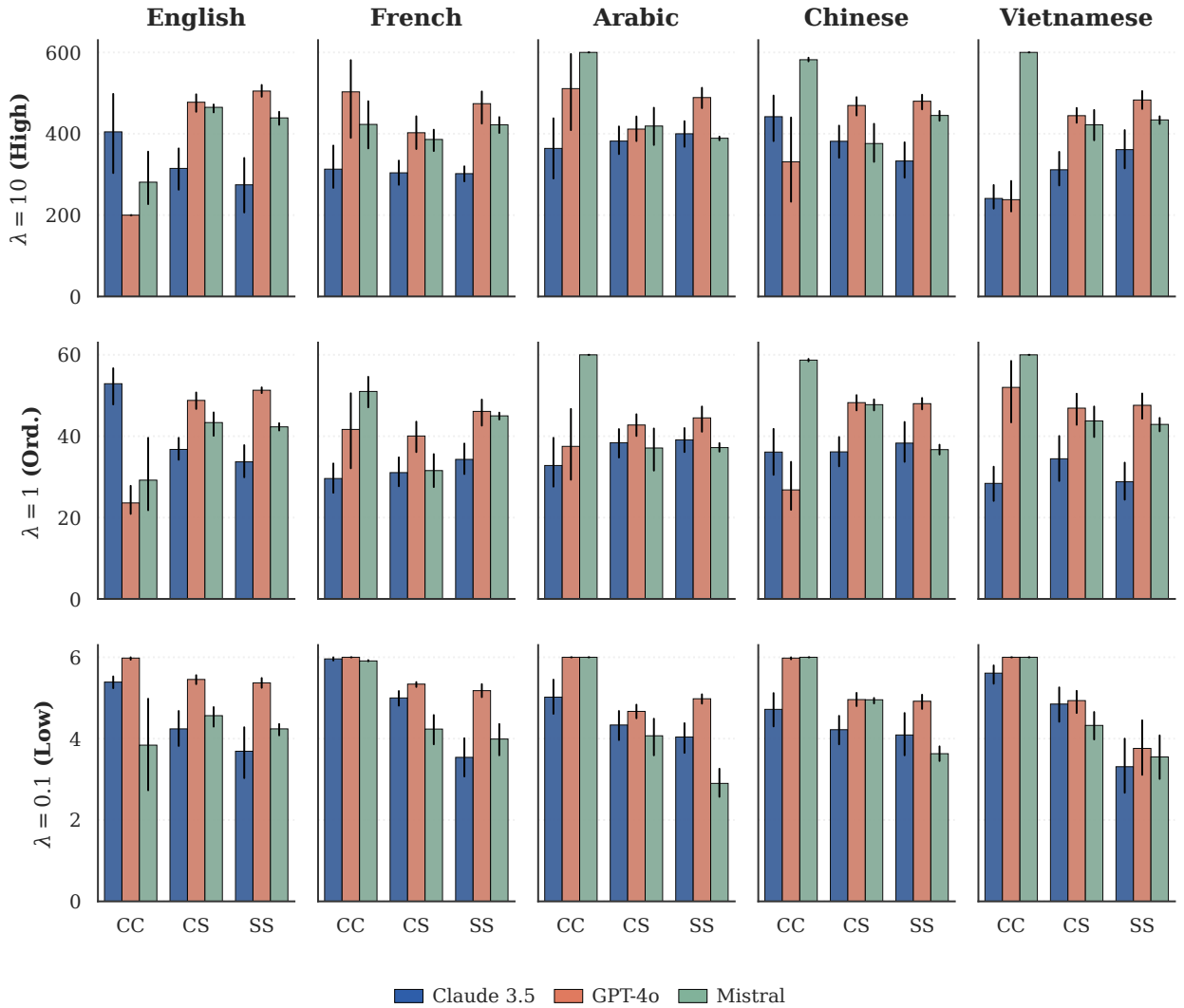


Figure 22: Aggregated final penalties across repeated Prisoner’s Dilemma games for the three proprietary LLMs (Claude 3.5 Haiku, GPT-4o, Mistral Large) under three payoff scales $\lambda \in \{0.1, 1.0, 10.0\}$. Results are reported across five languages (columns) and three personality pairings (CC, CS, SS, where CS pools the asymmetric CS and SC “mixed” pairings). Lower bars indicate better outcomes; error bars are bootstrap intervals over the repetitions within each displayed cell. The y-axis is rescaled by an order of magnitude across rows, mirroring the λ multiplier, so within-row comparison is the meaningful unit.

B.2. Mixed-strategy labels

The hybrid rule-based component of our classifier emits a *composite* label whenever a trajectory simultaneously satisfies the deterministic rule definitions of more than one canonical strategy (Appendix A.3). On the proprietary corpus at the $\tau \geq 0.9$ threshold, 75.6% of high-confidence trajectories receive a single canonical label and 24.4% receive a composite label. Table 10 reports the distribution of composite labels.

Table 10

Composite-label distribution among high-confidence ($\tau \geq 0.9$) proprietary trajectories that simultaneously satisfy more than one canonical rule. “Share of composite” is normalised within the composite subset; the composite subset itself accounts for 24.4% of all high-confidence trajectories.

Composite label	Count	Share of composite (%)
ALLD TFT	291	40.9
ALLC TFT WSLS	202	28.4
ALLD WSLS	122	17.1
TFT WSLS	97	13.6

The composite labels cluster around four patterns. The most frequent ALLD|TFT pattern corresponds to mutual-defection trajectories where the opponent also defects throughout: the agent’s all-defect history simultaneously satisfies ALLD and TFT, because TFT degenerates to ALLD when the opponent never cooperates. The next most frequent ALLC|TFT|WSLS triple is its mirror image: trajectories of nearly-all-cooperation that simultaneously satisfy ALLC, TFT and WSLS because the latter two strategies coincide with ALLC when no defection ever occurs. Both are structural ambiguities of short trajectories in absorbing mutual-cooperation or mutual-defection regimes rather than signs of genuine mixed play. ALLD|WSLS and TFT|WSLS reflect the well-known overlap between WSLS and other reactive strategies on short horizons under execution noise [14, 24, 42]. Removing the composite trajectories entirely or, alternatively, re-distributing them across their constituent labels under a uniform-mass tie-breaking rule shifts the aggregate frequencies in Table 1 by only a couple of percentage points per strategy and leaves the high-stake reversal documented in Section 3.5 unchanged.

B.3. Hidden Markov segmentation as a robustness check

To complement the rule-based composite-label diagnostic in Appendix B.2, we fit a four-state Hidden Markov Model on every proprietary trajectory. The four hidden states correspond to the four canonical strategies {ALLC, ALLD, TFT, WSLS}; the emission probability of state k at round t is the memory-one probability that strategy k produces the observed action given the joint history of round $t-1$, with a symmetric execution-noise factor $\epsilon=0.05$. The transition matrix is a uniform leak with switching probability 0.1 at every step. Viterbi decoding then returns the most likely sequence of hidden states.

Table 11

HMM Viterbi segmentation on the proprietary corpus ($n = 3,600$ trajectories): per- λ strategy share computed by redistributing each trajectory’s mass over the hidden states visited in its Viterbi path. The directional stake effect (ALLD share falling, ALLC share rising as λ grows from 0.1 to 1) is preserved.

λ	n	ALLC (%)	ALLD (%)	TFT (%)	WSLS (%)
0.1	1,200	35.16	47.98	8.33	8.53
1.0	1,200	50.12	28.34	8.40	13.13
10.0	1,200	51.38	29.82	9.09	9.71

Two key numbers stand out. First, only 20.2% of trajectories visit more than one hidden state, of the same order as the 24.4% composite-label rate of the rule-based pipeline (Appendix B.2); the small residual gap is consistent with the HMM’s smoothed Viterbi path being slightly less likely to flip between strategies than the strict rule-matching test. The average Viterbi path contains just 0.21 switches. Second, the redistributed per- λ shares in Table 11 reproduce the headline pattern of Section 3.2: ALLD share falls from 48% at $\lambda = 0.1$ to $\approx 30\%$ at $\lambda \in \{1, 10\}$, and ALLC absorbs most of the freed mass. The high-stake cooperation effect is therefore not an artefact of single-label attribution.

B.4. EGT detailed view across stakes and noise levels

Figures 23 and 24 unpack the two-panel summary in Figure 7 into the full per-strategy view. The first sweeps payoff scale λ on a logarithmic grid for three execution-noise levels and reports the stationary frequency of all four canonical strategies; the second holds λ fixed at three representative values and sweeps execution noise ϵ . Both are computed under identical settings ($Z = 100$, $\beta = 0.1$, $r = 10$ rounds, small-mutation limit).

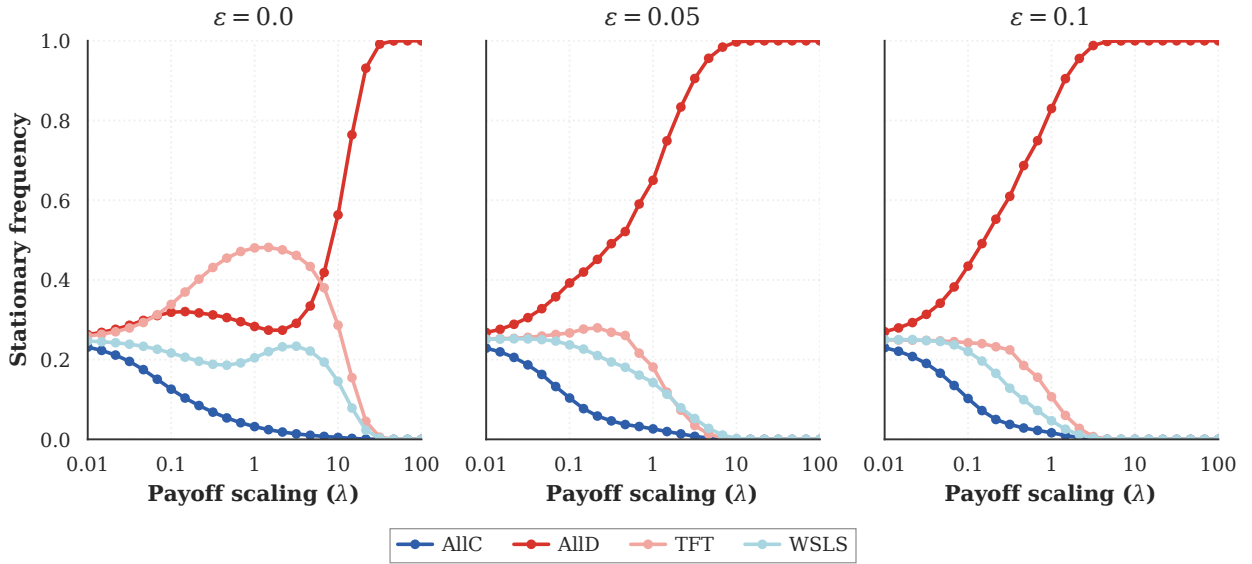
Strategy Frequency vs λ at $r=10$ ($\beta=0.1, Z=100$)


Figure 23: Stationary strategy frequencies as a function of payoff scaling λ for three execution-noise levels $\epsilon \in \{0, 0.05, 0.1\}$ at $r = 10$ rounds. Each panel reports the long-run frequency of the four canonical strategies (ALLC, ALLD, TFT, WSLS) in a finite well-mixed population ($Z = 100, \beta = 0.1$) under the small-mutation limit, using the FAIRGAME penalty matrix scaled by λ . ALLD becomes evolutionarily dominant as λ grows; introducing implementation noise accelerates the decay of TFT (sharply so at $\lambda = 1$) while the WSLS share decays more gradually, consistent with WSLS's self-correcting advantage.

At very low stakes ($\lambda \lesssim 0.1$) the conditional cooperators TFT and WSLS retain non-trivial mass because the payoff differential between mutual cooperation and mutual defection is too small for ALLD to invade efficiently. As λ grows, the relative advantage of ALLD against any partial cooperator widens and the stationary distribution sharply concentrates on ALLD, recovering the classical risk-dominant outcome predicted in finite populations. Modest implementation noise accelerates this collapse, and the effect is sharpest on TFT: at $\lambda = 1$ the TFT share falls from $\approx 48\%$ at $\epsilon = 0$ to $\approx 15\%$ at $\epsilon = 0.05$ and $\approx 9\%$ at $\epsilon = 0.1$, whereas the WSLS share decays more gradually over the same noise range, consistent with WSLS's self-correcting property of switching back to cooperation after mutual defection.

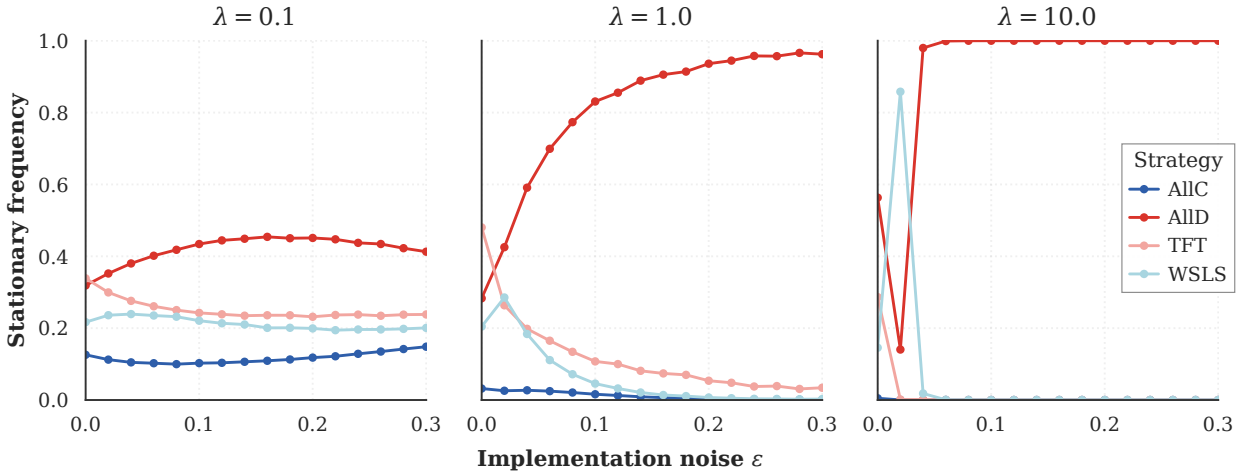
Strategy Frequency vs ε at $r=10$ ($\beta=0.1$, $Z=100$)


Figure 24: Stationary strategy frequencies as a function of execution noise ε for three payoff scales $\lambda \in \{0.1, 1, 10\}$ at $r = 10$ rounds. Population, selection intensity, and SML treatment are identical to those of Figure 23. At low stakes ($\lambda = 0.1$), execution noise erodes the conditional cooperators asymmetrically: TFT remains the modal conditional strategy across the whole noise range, but its share decays by ≈ 11 percentage points as ε goes from 0 to 0.3, while the WSLS share stays roughly flat (≈ 22 – 26%); the freed mass migrates to ALLD. At higher stakes ($\lambda \in \{1, 10\}$), the population is locked into ALLD irrespective of ε .

Holding λ fixed and sweeping ε makes the noise-tolerance asymmetry directly visible: at $\lambda = 0.1$, where ALLD is least dominant, increasing ε erodes the conditional cooperators with a steeper drop on TFT than on WSLS, and the freed mass migrates to ALLD; at $\lambda \in \{1, 10\}$ the population is locked into ALLD regardless of ε .

B.5. Baseline FAIRGAME analysis: detailed results

This appendix presents the complete analysis of LLM strategic behaviour from the baseline FAIRGAME dataset, complementing the payoff-scaled experiments in the main text. The dataset covers four LLM models - Claude 3.5 Sonnet, Llama 3.1 405B Instruct, Mistral Large, and GPT-4o - across five languages (Arabic, Chinese, English, French, and Vietnamese).

B.5.1. Hybrid classification approach

While our LSTM model demonstrates strong performance in strategy classification, it was originally designed as a single-label classifier. To address this limitation and ensure comprehensive coverage, we adopt a hybrid labelling approach that combines model predictions with rule-based strategy assignment (see Appendix A.3).

B.5.2. Strategy distribution across models

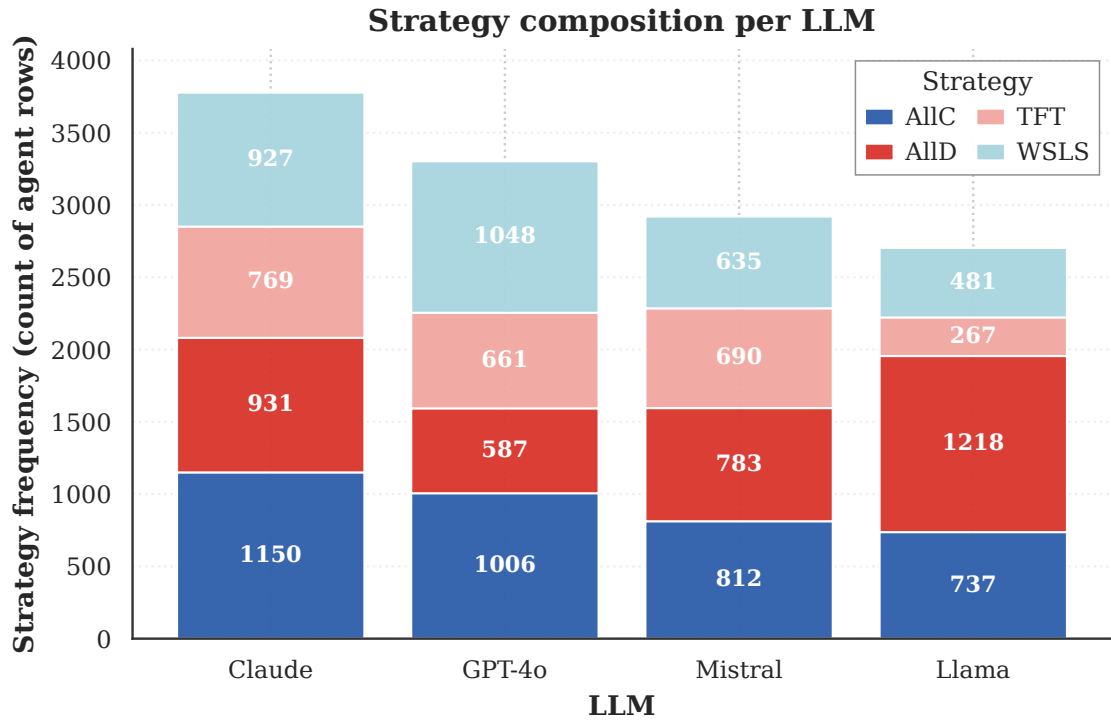


Figure 25: Strategic behavioural composition of four LLMs in the iterated Prisoner’s Dilemma. Each stacked column shows the absolute count of agent–game rows assigned to each strategy by the hybrid LSTM + rule-based classifier on the baseline FAIRGAME corpus (1,200 games per model \times 2 agents per game = 2,400 base rows; composite labels such as “ALLD|WSLS” are expanded into one row per component, yielding the totals annotated on each bar).

The strategic preference analysis from the *baseline FAIRGAME dataset* (4,800 games pooled across four models, 12,702 rows after composite expansion) reveals heterogeneity in decision-making across LLM architectures. Claude 3.5 Sonnet is mildly cooperative-leaning but otherwise balanced: ALLC (30.4%) is the modal strategy, with ALLD (24.6%), WSLS (24.5%) and TFT (20.4%) all within five percentage points of each other. Llama 3.1 405B Instruct is the only defection-dominant model: ALLD (45.1%) accounts for nearly half of its rows, while TFT (9.9%) and WSLS (17.8%) are correspondingly suppressed. Mistral Large produces the flattest distribution of any model in our corpus, with the four strategies occupying 27.8% (ALLC), 26.8% (ALLD), 23.6% (TFT) and 21.7% (WSLS). Finally, GPT-4o is the most reciprocity-tilted: WSLS (31.7%) and ALLC (30.5%) jointly account for 62.2% of its rows, with ALLD held to 17.8%.¹

¹GPT-4o exhibits a markedly higher ALLD share in the payoff-scaled experiments of the main paper, where stake magnitude rather than language is the manipulation of interest. The baseline corpus reported here fixes λ at the FAIRGAME default and therefore captures a different operating point of the same model.

B.5.3. Language effects on strategies

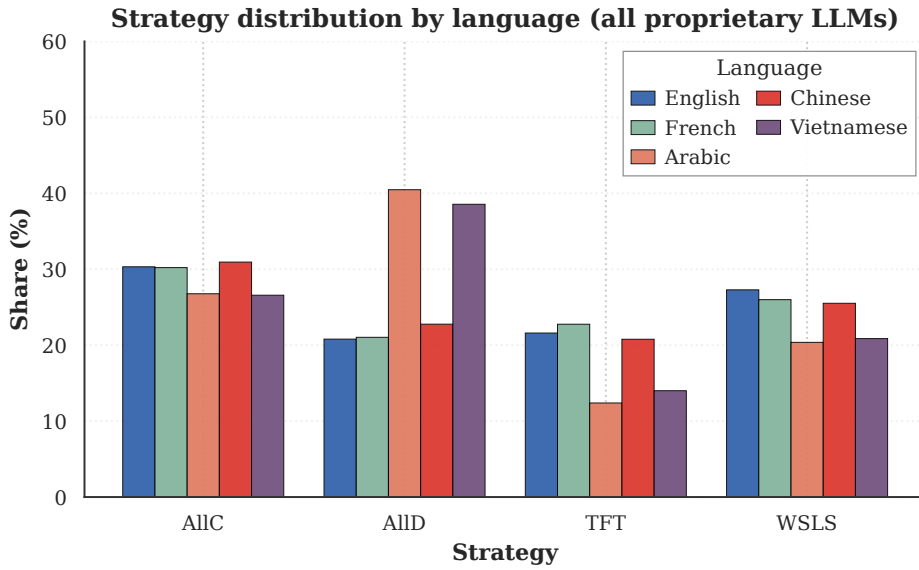


Figure 26: Strategy distribution across languages on the baseline FAIRGAME dataset, pooled across all four proprietary LLMs. Arabic and Vietnamese stand apart with markedly higher ALLD shares, while English, French and Chinese cluster together at much lower defection rates.

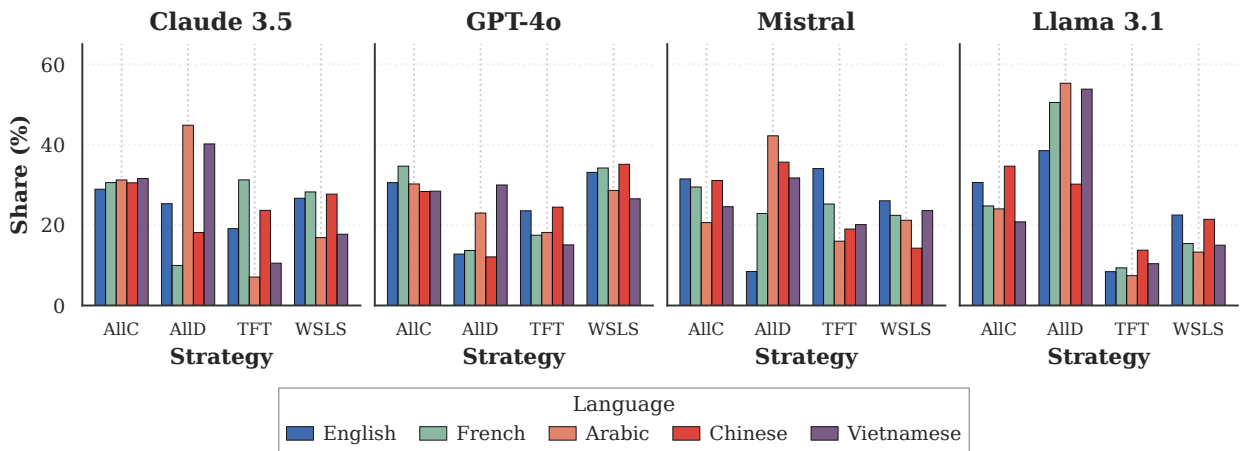


Figure 27: Strategy distribution by language, faceted per LLM (Claude 3.5, GPT-4o, Mistral, Llama 3.1 405B). The Arabic/Vietnamese vs. English/French/Chinese cluster split observed in Figure 26 is reproduced inside every model, so it is not driven by any single LLM’s idiosyncrasies.

The language of the interaction has a substantial and direction-consistent effect on the strategic mix. Pooling all four models, the five languages split into two clusters along the defection axis: Arabic (40.5% ALLD) and Vietnamese (38.6% ALLD) sit roughly twenty percentage points above English (20.8%), French (21.0%) and Chinese (22.8%), which are statistically indistinguishable from each other on this metric. The same cluster boundary reappears, with mirror symmetry, in the conditional strategies: English (27.3% WSLS, 21.6% TFT), French (26.0%, 22.8%) and Chinese (25.5%, 20.8%) all carry between forty and fifty percent of their probability mass on the two reciprocal strategies, whereas Arabic (20.4%, 12.4%) and Vietnamese (20.9%, 14.0%) carry only about a third. The unconditional cooperation share is far less language-sensitive, ranging only from 26.6% (Vietnamese) to 30.9% (Chinese). Figure 27 shows that this two-cluster pattern is reproduced inside every model, so it is not driven by any one LLM’s idiosyncrasies.

B.5.4. Strategy recognition via supervised machine learning

The language effect (baseline dataset). *The following analysis is restricted to the baseline FAIRGAME dataset (Claude 3.5 Sonnet, Llama 3.1 405B, GPT-4o, Mistral Large) and is independent of the payoff-scaled experiments in the main paper; the language patterns reported here are baseline-corpus effects.*

Figure 28 combines two complementary views of the language effect. Panel (a) reports the per-agent total score (sum of per-round penalties) averaged across all games in each language. Two regularities stand out. First, Agent 2 outperforms Agent 1 in every language; the average gap is 9.0 penalty points and is largest in Arabic (12.0) and English (12.0), suggesting a structural second-mover advantage in the FAIRGAME prompt template. Second, the language-by-language ordering of agent payoffs is itself informative: Arabic (47.79 / 59.82) and Vietnamese (49.99 / 55.69) yield the highest absolute scores – consistent with the elevated ALLD rates documented in Figure 26 above, since defection is the higher-payoff strategy in a one-shot Prisoner’s Dilemma – while English (41.41 / 53.37) and French (41.90 / 51.33) yield the lowest, consistent with their higher conditional-cooperation rates.

Panel (b) shows the same strategy-by-language crosstab as the top sub-panel of Figure 26 and confirms two structural patterns. (i) The languages cluster into a “defection-leaning” bloc (Arabic, Vietnamese: ALLD \approx 40%) and a “reciprocity-leaning” bloc (English, French, Chinese: ALLD \approx 21%); the gap on this single axis is approximately twenty percentage points. (ii) Within the reciprocity-leaning bloc, the three languages are nearly interchangeable – their WLSL shares lie in a narrow 25.5–27.3% band and their TFT shares in 20.8–22.8% – so any individual claim of a uniquely “Chinese TFT” or “French WLSL” signature would be unsupported by these data. Unconditional cooperation (ALLC), by contrast, is essentially flat across languages (26.6–30.9%), so the language effect operates mainly through the conditional/unconditional defection trade-off rather than through cooperative behaviour per se. These findings indicate that the prompt language modulates whether the model retrieves a contingent-reciprocity or a one-shot defection script, rather than uniformly tilting it toward cooperation or competition.

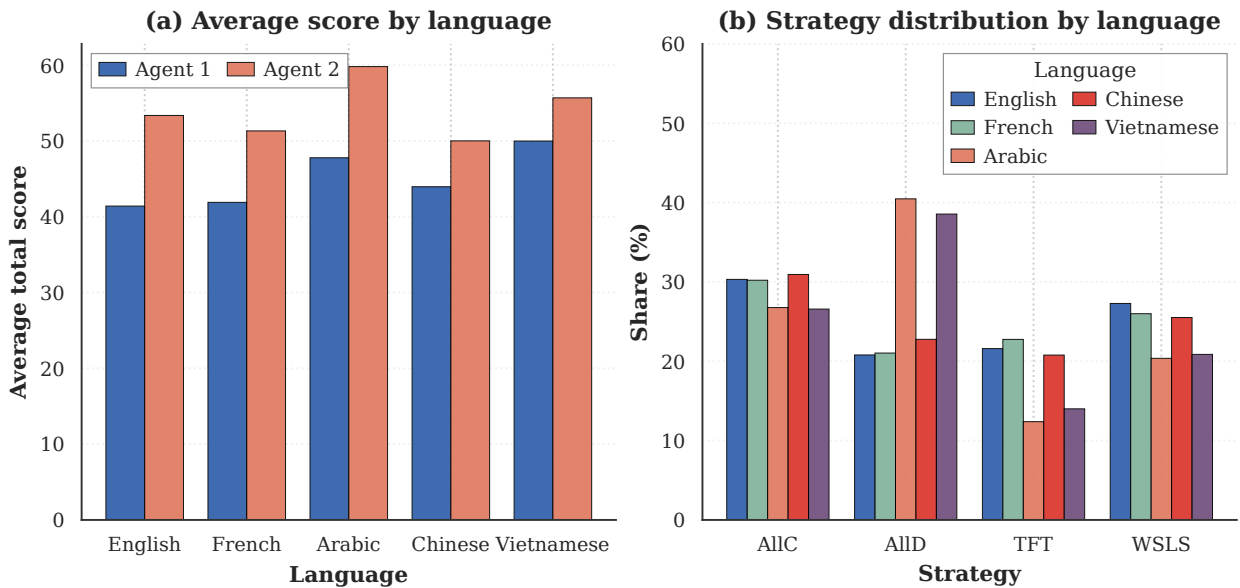


Figure 28: The language effect. (a) Mean cumulative per-agent score by prompt language (sum of per-round penalties; higher = more total payoff). Agent 2 outperforms Agent 1 in every language, and absolute scores are highest in Arabic and Vietnamese – the same languages that elicit the highest ALLD rates in panel (b). (b) Strategy distribution by language pooled across all four LLMs: Arabic and Vietnamese cluster apart from English, French and Chinese on the ALLD axis, while ALLC is approximately language-invariant.

B.6. Open-weight small LLMs: robustness checks

Four follow-up analyses substantiate the open-weight small-LLM results reported in Section 3.6. They are grouped here for clarity: the per-condition penalty breakdown provides the full cell-level view of mean penalties across languages and personality pairings; horizon robustness checks that the directional stake effect is detectable already

in the first ten rounds; confidence-threshold robustness checks that the model-level heterogeneity is not driven by the $\tau = 0.9$ cutoff; and the chi-square test quantifies the stake effect on this corpus.

B.6.1. Per-condition penalty breakdown (open-weight small LLMs)

The companion of Figure 22 for the open-weight small LLMs: Figure 29 reports the per-cell mean penalties at the three stake regimes that match the proprietary analysis ($\lambda \in \{0.1, 1, 10\}$). The picture is qualitatively similar: cooperative pairings (CC) consistently incur lower penalties than selfish ones (SS); per-language differences are model-specific; and the Arabic prompts again elicit elevated defection in cooperative pairings.

Payoff scaling shapes cooperation in LLM agents across languages

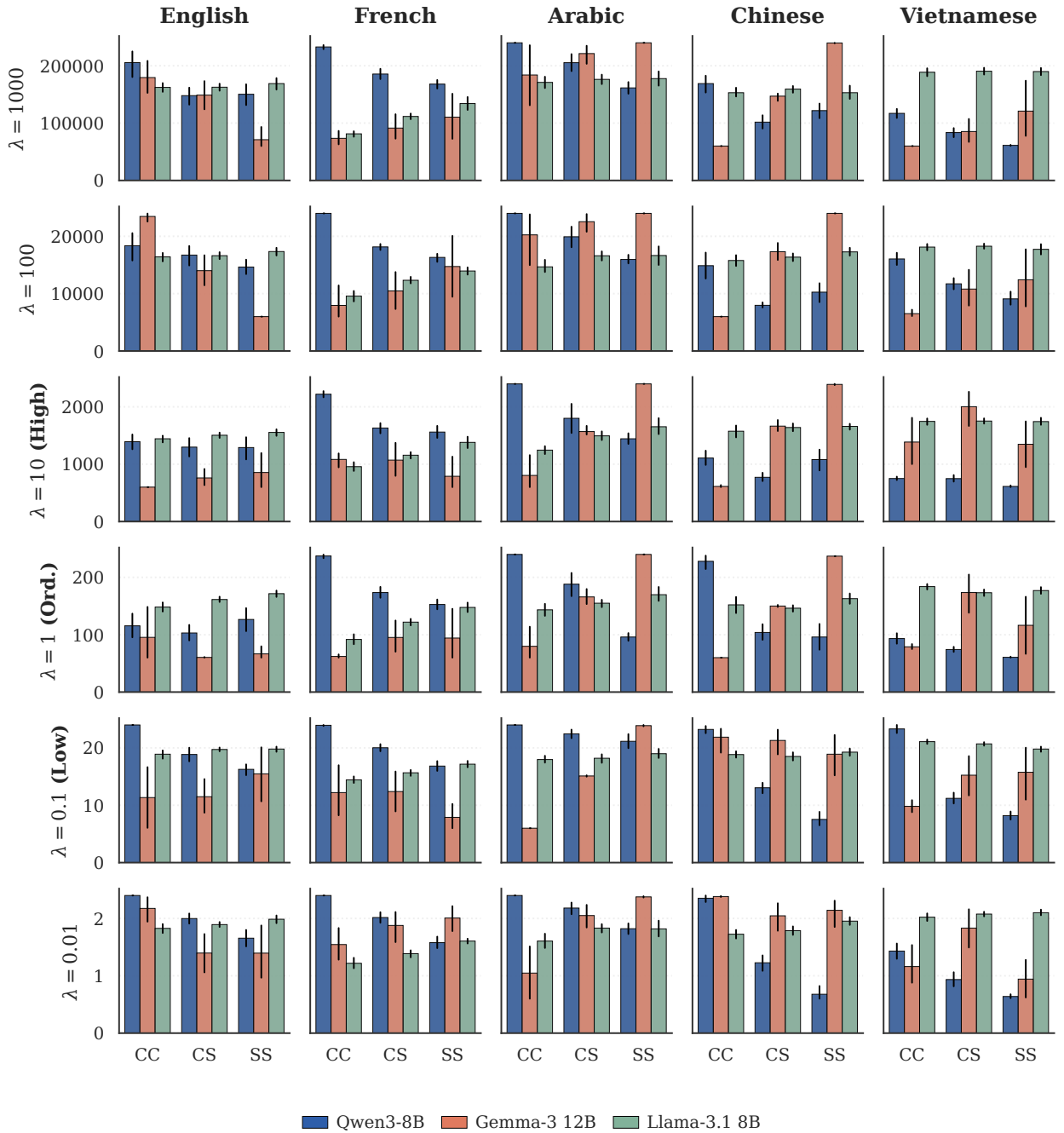


Figure 29: Per-condition penalties for the three open-weight LLMs under the payoff-scaled Prisoner’s Dilemma. Rows group three stake regimes (**High:** $\lambda=10$; **Ordinary:** $\lambda=1$; **Very low:** $\lambda=0.1$); columns correspond to the prompt language; within each panel the x -axis lists the personality pairing (CC, CS, SS, where CS pools the asymmetric CS and SC “Mixed” pairings) and the three bars give the per-agent mean penalty for Qwen3 8B (blue), Gemma-3 12B (orange) and Llama-3.1 8B (green). Lower bars indicate better outcomes; error bars are bootstrap intervals over the repetitions within each displayed cell. The y -axis is rescaled by an order of magnitude across rows, mirroring the λ multiplier, so within-row comparison is the meaningful unit.

B.6.2. Horizon robustness

The open-weight small-LLM runs reported in Section 3.6 use $N=30$ rounds, while the proprietary-model runs in Section 3.1 use $N=10$. To verify that the directional stake effect identified in the open-weight corpus is detectable already in the first ten rounds – and thus that the proprietary-vs-small comparison reported in Section 3.6 is not driven by horizon length – we apply the same strict rule-based classifier of Appendix A.3 to two parallel sequences for every open-weight agent: the truncated trajectory (rounds 1–10 only) and the full trajectory (rounds 1–30). Table 12 reports the resulting per- λ distributions, pooled across the three open-weight models and five languages.

Table 12

Rule-based strategy distribution (%) for the open-weight small LLMs computed on the first 10 rounds (“ $N=10$ ”) versus the full 30 rounds (“ $N=30$ ”) of every agent trajectory. “NONE” denotes trajectories that do not satisfy any canonical rule with tolerance $\epsilon_{\text{noise}}=0.1$. The truncated and full classifications agree on 85.7% of trajectories overall, and the directional stake effect (ALLD share falling and ALLC share rising as λ grows from 0.1 to 10) appears already at $N=10$.

λ	Horizon	ALLC	ALLD	TFT	WSLS	NONE	n
0.1	$N=10$	32.15	47.81	2.16	0.79	17.09	1527
	$N=30$	33.79	37.66	1.77	0.85	25.93	
1.0	$N=10$	53.06	25.63	1.62	0.72	18.97	1666
	$N=30$	56.72	22.51	0.48	0.18	20.11	
10.0	$N=10$	50.80	26.79	1.09	0.90	20.41	1553
	$N=30$	53.25	21.57	2.45	0.19	22.54	

Two observations follow. First, the per-trajectory label assigned on the first 10 rounds agrees with the label assigned on the full 30 rounds in 85.7% of cases, indicating that the rule-based classifier is largely horizon-stable on these data. Second, the qualitative pattern of the stake effect – ALLD share dropping by approximately 20 percentage points between $\lambda=0.1$ and $\lambda=1$, and remaining at a similar level at $\lambda=10$ – is reproduced almost identically by the truncated and full classifications. The directional comparison with the proprietary-model corpus reported in Section 3.6 and Figure 13 is therefore not an artefact of horizon length. The slightly higher share of “NONE” (unclassifiable) trajectories at $N=30$ is consistent with longer sequences accumulating execution errors that push them outside the canonical rule envelopes, an effect that the LSTM-based hybrid pipeline used in the main text actively absorbs via its noise tolerance.

B.6.3. Confidence-threshold robustness

For completeness, Figure 30 reports the unfit-trajectory rate as a function of the LSTM-output confidence threshold τ , computed separately for Qwen3 8B, Gemma-3 12B and Llama-3.1 8B on the open-weight payoff-scaled corpus. At the $\tau = 0.9$ threshold used in the main analysis, the unfit rate stays below 30% for Gemma-3 12B and Qwen3 8B and below 50% for Llama-3.1 8B; the qualitative ordering of models by conditional-cooperation capacity reported in Section 3.6 is preserved across the entire $\tau \in [0.6, 0.95]$ range, confirming that the threshold choice is not the driver of the model-level heterogeneity.

Model Uncertainty vs Confidence Threshold

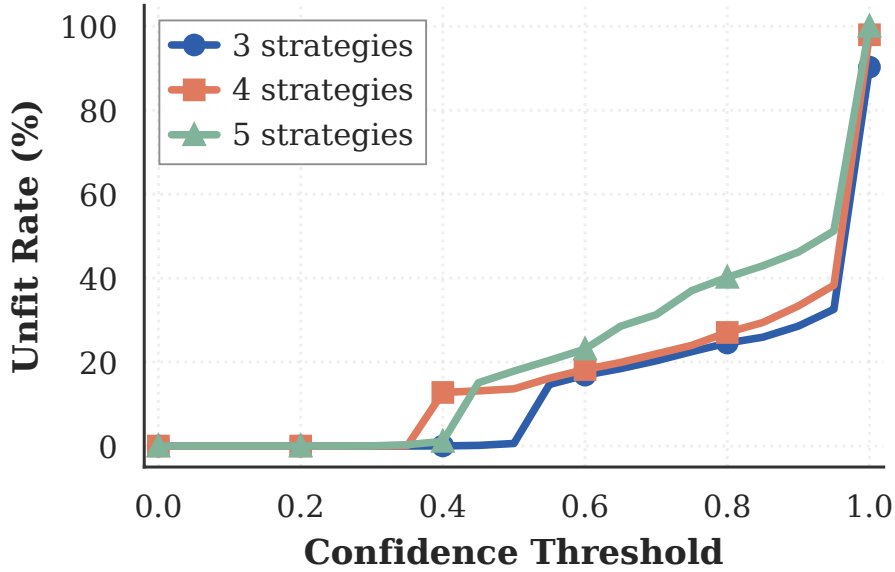


Figure 30: Unfit (non-classifiable) trajectory rate as a function of the LSTM-output confidence threshold τ for the three open-weight small LLMs. The vertical line at $\tau=0.9$ marks the threshold used in the main analysis. Llama-3.1 8B has the largest unfit rate at all τ , consistent with its noisier conditional play.

B.6.4. Chi-square stake-effect test

Table 13 reports the chi-square test of independence between inferred strategy and stake λ for the open-weight small LLMs, both pooled and per model. The test is run on $\tau > 0.9$ high-confidence trajectories at all six multipliers $\lambda \in \{0.01, 0.1, 1, 10, 100, 1000\}$, parallel in spirit to the proprietary-corpus test in Section 3.3. The pooled effect size (Cramér’s $V \approx 0.10$) is larger than the value observed in the proprietary corpus restricted to three lambdas ($V \approx 0.065$), reflecting the wider stake sweep used here. Per-model, Gemma-3 12B is the least stake-sensitive, consistent with its early-commitment trajectory shape; Llama-3.1 8B is the most sensitive, reflecting its sharp moves between defection-leaning and Tit-for-Tat-dominated regimes; Qwen3 8B sits in between, with the U-shape stake response we noted in the main text.

Table 13

Chi-square test of independence between inferred strategy and stake λ for the open-weight small LLMs at $\tau \geq 0.9$, computed over the full six-multiplier sweep $\lambda \in \{0.01, 0.1, 1, 10, 100, 1000\}$ on the canonical cache (composite labels expanded into one row per matched strategy, identically to Tables 5 and 6). Effect sizes are reported as Cramér’s V .

Scope	n	χ^2	dof	p -value	Cramér’s V
Gemma-3 12B	4,663	131.16	15	1.3×10^{-20}	0.097
Qwen3 8B	2,973	143.35	15	5.0×10^{-23}	0.127
Llama-3.1 8B	1,621	227.65	15	4.9×10^{-40}	0.216
Pooled	9,257	274.90	15	9.0×10^{-50}	0.099

CRedit authorship contribution statement

Trung-Kiet Huynh: . Dao-Sy Duy-Minh: . Thanh-Bang Cao: . Phong-Hao Le: . Hong-Dan Nguyen: . Phu-Quy Nguyen-Lam: . Minh-Luan Nguyen-Vo: . Hong-Phat Pham: . Phu-Hoa Pham: . Thien-Kim Than: . Chi-Nguyen Tran: . Huy Tran: . Gia-Thoai Tran-Le: . Alessio Buscemi: . Le Hong Trang: . The Anh Han: .

References

- [1] Akata, E., Schulz, L., Coda-Forno, J., Oh, S.J., Bethge, M., Schulz, E., 2025. Playing repeated games with large language models. *Nature Human Behaviour* 9, 1380–1390. doi:10.1038/s41562-025-02172-y.
- [2] Anh, H.T., Moniz Pereira, L., Santos, F.C., 2011. Intention recognition promotes the emergence of cooperation. *Adaptive Behavior* 19, 264–279.
- [3] Anthropic, 2024. Introducing computer use, a new Claude 3.5 Sonnet, and Claude 3.5 Haiku. <https://www.anthropic.com/news/3-5-models-and-computer-use>. Accessed: 2026-04-28.
- [4] Axelrod, R., 1980. More effective choice in the prisoner's dilemma. *The Journal of Conflict Resolution* 24, 379–403. URL: <http://www.jstor.org/stable/173638>, doi:10.1177/002200278002400301.
- [5] Backmann, S., Guzman Piedrahita, D., Tewolde, E., Mihalcea, R., Schölkopf, B., Jin, Z., 2025. When ethics and payoffs diverge: LLM agents in morally charged social dilemmas. *arXiv:2505.19212*. preprint.
- [6] Bai, Y., Kadavath, S., Kundu, S., Askell, A., Kernion, J., Jones, A., Chen, A., Goldie, A., Mirhoseini, A., McKinnon, C., et al., 2022. Constitutional ai: Harmlessness from ai feedback. *arXiv preprint arXiv:2212.08073* URL: <https://arxiv.org/abs/2212.08073>.
- [7] Balabanova, N., Bashir, A., Bova, P., Buscemi, A., Cimpeanu, T., da Fonseca, H.C., Di Stefano, A., Duong, M.H., Fernández Domingos, E., Fernandes, A.M., Han, T.A., Krellner, M., Ogbo, N.B., Powers, S.T., Proverbio, D., Santos, F.P., Shamszaman, Z.U., Song, Z., 2025. Media and responsible AI governance: a game-theoretic and LLM analysis. *Philosophical Transactions of the Royal Society A* In press.
- [8] Breiman, L., 2001. Random forests. *Mach. Learn.* 45, 5–32. URL: <https://doi.org/10.1023/A:1010933404324>, doi:10.1023/A:1010933404324.
- [9] Buscemi, A., Proverbio, D., Bova, P., Balabanova, N., Bashir, A., Cimpeanu, T., et al., 2025a. Do LLMs trust AI regulation? Emerging behaviour of game-theoretic LLM agents. *arXiv:2504.08640*.
- [10] Buscemi, A., Proverbio, D., Di Stefano, A., Han, T.A., Castignani, G., Liò, P., 2025b. FAIRGAME: a framework for AI agents bias recognition using game theory, in: *ECAI 2025 – Proceedings of the 28th European Conference on Artificial Intelligence*, IOS Press. pp. 4097–4104. doi:10.3233/FAIA251300.
- [11] Buscemi, A., Proverbio, D., Di Stefano, A., Han, T.A., Castignani, G., Liò, P., 2025c. Strategic communication and language bias in multi-agent llm coordination, in: *International Conference on Multi-disciplinary Trends in Artificial Intelligence*, Springer. pp. 289–301.
- [12] Cook, A., Karakuş, O., 2024. Llm-commentator: Novel fine-tuning strategies of large language models for automatic commentary generation using football event data. *Knowledge-Based Systems* 300, 112219.
- [13] Cox, D.R., 1958. The regression analysis of binary sequences. *Journal of the Royal Statistical Society: Series B (Methodological)* 20, 215–232. doi:10.1111/j.2517-6161.1958.tb00292.x.
- [14] Di Stefano, A., Jayne, C., Angione, C., Han, T.A., 2023. Recognition of behavioural intention in repeated games using machine learning, in: *Artificial Life Conference Proceedings 35*, MIT Press. p. 103.
- [15] Domingos, E.F., Santos, F.C., Lenaerts, T., 2023. Egttools: Evolutionary game dynamics in python. *Iscience* 26.
- [16] Fan, C., Chen, J., Jin, Y., He, H., 2024. Can large language models serve as rational players in game theory? a systematic analysis, in: *Proc. AAAI Conference on Artificial Intelligence*, pp. 17960–17967.
- [17] Fontana, N., Pierri, F., Aiello, L.M., 2025. Nicer than humans: How do large language models behave in the prisoner's dilemma?, in: *Proceedings of the International AAAI Conference on Web and Social Media (ICWSM)*, pp. 522–535. URL: <https://ojs.aaai.org/index.php/ICWSM/article/view/35829>, doi:10.1609/icws.v19i1.35829.
- [18] Fu, F., Chen, X., Christakis, N.A., 2026. On the optimal integration of intelligent agents into network systems to steer cooperation. *Proceedings of the National Academy of Sciences* 123, e2537939123.
- [19] Fujimoto, Y., Kaneko, K., 2019. Functional dynamics by intention recognition in iterated games. *New Journal of Physics* 21, 023025. doi:10.1088/1367-2630/ab0459.
- [20] Gemma Team, Google DeepMind, 2025. Gemma 3 technical report. *arXiv:2503.19786*. preprint.
- [21] Hammond, L., Chan, A., Clifton, J., Hoelscher-Obermaier, J., Khan, A., McLean, E., Smith, C., Barfuss, W., Foerster, J., Gavenčiak, T., et al., 2025. Multi-Agent Risks from Advanced AI. *arXiv preprint arXiv:2502.14143*.
- [22] Han, T.A., Leibo, J.Z., Lenaerts, T., Rahwan, I., Santos, F., Perc, M., Capraro, V., 2026. Social physics in the age of artificial intelligence. *arXiv preprint arXiv:2603.16900*.
- [23] Han, T.A., Pereira, L.M., Santos, F.C., 2011. The role of intention recognition in the evolution of cooperative behavior, in: *Proceedings of the Twenty-Second international joint conference on Artificial Intelligence (IJCAI)*, pp. 1684–1689.
- [24] Han, T.A., Pereira, L.M., Santos, F.C., 2012. Corpus-based intention recognition in cooperation dilemmas. *Artificial Life* 18, 365–383. URL: https://doi.org/10.1162/ARTL_a_00072, doi:10.1162/ARTL_a_00072.
- [25] Han, T.A., Perret, C., Powers, S.T., 2021. When to (or not to) trust intelligent machines: Insights from an evolutionary game theory analysis of trust in repeated games. *Cognitive Systems Research* 68, 111–124. URL: <https://doi.org/10.1016/j.cogsys.2021.02.003>, doi:10.1016/j.cogsys.2021.02.003.
- [26] Hilbe, C., Nowak, M.A., Sigmund, K., 2013. Evolution of extortion in Iterated Prisoner's Dilemma games. *Proceedings of the National Academy of Sciences* 110, 6913–6918. doi:10.1073/pnas.1214834110.
- [27] Hochreiter, S., Schmidhuber, J., 1997. Long short-term memory. *Neural Computation* 9, 1735–1780. URL: <https://doi.org/10.1162/neco.1997.9.8.1735>, doi:10.1162/neco.1997.9.8.1735.
- [28] Hua, W., Liu, O., Li, L., Amayuelas, A., Chen, J., Jiang, L., et al., 2024. Game-theoretic LLM: Agent workflow for negotiation games. URL: <https://arxiv.org/abs/2411.05990>, *arXiv:2411.05990*.
- [29] Hurst, A., Lerer, A., Goucher, A.P., et al., 2024. GPT-4o system card. URL: <https://arxiv.org/abs/2410.21276>, *arXiv:2410.21276*.
- [30] Idowu, J., Almasoud, A., Alfahid, A., 2026. Mapping human anti-collusion mechanisms to multi-agent ai systems. *Knowledge-Based Systems*, 116067.
- [31] Imhof, L.A., Fudenberg, D., Nowak, M.A., 2007. Tit-for-tat or win-stay, lose-shift? *Journal of theoretical biology* 247, 574–580.

- [32] Jordan, M.I., Bishop, C.M., 1996. Neural networks. *ACM Comput. Surv.* 28, 73–75. URL: <https://doi.org/10.1145/234313.234348>, doi:10.1145/234313.234348.
- [33] Krockow, E.M., Colman, A.M., Pulford, B.D., 2016. Cooperation in repeated interactions: A systematic review of centipede game experiments, 1992–2016. *European Review of Social Psychology* 27, 231–282.
- [34] List, J.A., 2006. Friend or foe? a natural experiment of the prisoner’s dilemma. *The Review of Economics and Statistics* 88, 463–471.
- [35] Liu, L., Chen, X., 2020. Evolutionary game dynamics in multiagent systems with prosocial and antisocial exclusion strategies. *Knowledge-Based Systems* 188, 104835.
- [36] Llama Team, AI @ Meta, 2024. The Llama 3 herd of models. [arXiv:2407.21783](https://arxiv.org/abs/2407.21783). preprint.
- [37] Lorè, N., Heydari, B., 2024. Strategic behavior of large language models and the role of game structure versus contextual framing. *Scientific Reports* 14, 18490. URL: <https://www.nature.com/articles/s41598-024-69032-z>, doi:10.1038/s41598-024-69032-z.
- [38] Lorè, N., Heydari, B., 2026. Communication enhances LLMs’ stability in strategic thinking. [arXiv:2602.06081](https://arxiv.org/abs/2602.06081). preprint.
- [39] Lu, Y., Aleta, A., Du, C., Shi, L., Moreno, Y., 2024. LLMs and generative agent-based models for complex systems research. *Physics of Life Reviews* 51, 283–293. doi:10.1016/j.plrev.2024.10.013.
- [40] Mao, S., Cai, Y., Xia, Y., Wu, W., Wang, X., Wang, F., Guan, Q., Ge, T., Wei, F., 2025. Alympics: Llm agents meet game theory, in: *Proceedings of the 31st International Conference on Computational Linguistics*, pp. 2845–2866.
- [41] Mistral AI, 2024. Large enough: Mistral Large 2. <https://mistral.ai/news/mistral-large-2407>. Accessed: 2026-04-28.
- [42] Montero-Porras, E., Grujić, J., Fernández Domingos, E., Lenaerts, T., 2022. Inferring strategies from observations in long iterated prisoner’s dilemma experiments. *Scientific Reports* 12. doi:10.1038/s41598-022-11654-2.
- [43] Nowak, M.A., Sasaki, A., Taylor, C., Fudenberg, D., 2004. Emergence of cooperation and evolutionary stability in finite populations. *Nature* 428, 646–650.
- [44] Ouyang, L., Wu, J., Jiang, X., Almeida, D., Wainwright, C., Mishkin, P., Zhang, C., Agarwal, S., Slama, K., Ray, A., et al., 2022. Training language models to follow instructions with human feedback. *Advances in Neural Information Processing Systems* 35, 27730–27744. URL: <https://arxiv.org/abs/2203.02155>.
- [45] Pal, S., Mallela, A., Hilbe, C., Pracher, L., Wei, C., Fu, F., Schnell, S., Nowak, M.A., 2026. Strategies of cooperation and defection in five large language models. [arXiv preprint https://arxiv.org/abs/2601.09849](https://arxiv.org/abs/2601.09849) [arXiv:2601.09849](https://arxiv.org/abs/2601.09849).
- [46] Pires, A.S., Samson, L., Ghebrea, S., Santos, F.P., 2025. How large language models judge and influence human cooperation. [arXiv preprint arXiv:2507.00088](https://arxiv.org/abs/2507.00088).
- [47] Press, W.H., Dyson, F.J., 2012. Iterated prisoner’s dilemma contains strategies that dominate any evolutionary opponent. *Proceedings of the National Academy of Sciences* 109, 10409–10413. doi:10.1073/pnas.1206569109.
- [48] Qwen Team, 2025. Qwen3 technical report. [arXiv:2505.09388](https://arxiv.org/abs/2505.09388). preprint.
- [49] Rand, D.G., Tarnita, C.E., Ohtsuki, H., Nowak, M.A., 2013. Evolution of fairness in the one-shot anonymous ultimatum game. *Proceedings of the National Academy of Sciences* 110, 2581–2586.
- [50] Sigmund, K., 2010. *The calculus of selfishness*. Princeton Univ. Press.
- [51] Sun, H., Wu, Y., Cheng, Y., Chu, X., 2025. Game theory meets large language models: A systematic survey, in: *Proceedings of the Thirty-Fourth International Joint Conference on Artificial Intelligence (IJCAI-25), Survey Track*, pp. 10669–10677. URL: <https://www.ijcai.org/proceedings/2025/1184>, doi:10.24963/ijcai.2025/1184.
- [52] Szabó, G., Tóke, C., 1998. Evolutionary prisoner’s dilemma game on a square lattice. *Physical Review E* 58, 69.
- [53] Tessler, M.H., Bakker, M.A., Jarrett, D., Sheahan, H., Chadwick, M.J., et al., 2024. Ai can help humans find common ground in democratic deliberation. *Science* 386, eadq2852.
- [54] Tewolde, E., Zhang, X., Guzman Piedrahita, D., Conitzer, V., Jin, Z., 2026. CoopEval: Benchmarking cooperation-sustaining mechanisms and LLM agents in social dilemmas. [arXiv:2604.15267](https://arxiv.org/abs/2604.15267). preprint.
- [55] Willis, R., Du, Y., Leibo, J.Z., 2025. Will systems of llm agents lead to cooperation: An investigation into a social dilemma, in: *Proceedings of the 24th International Conference on Autonomous Agents and Multiagent Systems*, pp. 2786–2788.
- [56] Zisis, I., Di Guida, S., Han, T.A., Kirchsteiger, G., Lenaerts, T., 2015. Generosity motivated by acceptance-evolutionary analysis of an anticipation game. *Scientific reports* 5, 18076.